

On the Performance of Downlink NOMA in Underlay Spectrum Sharing

Vaibhav Kumar, *Member, IEEE*, Zhiguo Ding, *Fellow, IEEE*, and Mark F. Flanagan, *Senior Member, IEEE*

Abstract—Non-orthogonal multiple access (NOMA) and spectrum sharing are two potential technologies for providing massive connectivity in beyond fifth-generation (B5G) networks. In this paper, we present the performance analysis of a multi-antenna-assisted two-user downlink NOMA system in an underlay spectrum sharing system. We derive closed-form expressions for the average achievable sum-rate and outage probability of the secondary network under a peak interference constraint and/or peak power constraint, depending on the availability of channel state information (CSI) of the interference link between secondary transmitter (ST) and primary receiver (PR). For the case where the ST has a fixed power budget, we show that performance can be divided into two specific regimes, where either the interference constraint or the power constraint primarily dictates the performance. Our results confirm that the NOMA-based underlay spectrum sharing system significantly outperforms its orthogonal multiple access (OMA) based counterpart, by achieving higher average sum-rate and lower outage probability. We also show the effect of information loss at the ST in terms of CSI of the link between the ST and PR on the system performance. Moreover, we also present closed-form expressions for the optimal power allocation coefficient that minimizes the outage probability of the NOMA system for the special case where the secondary users are each equipped with a single antenna. A close agreement between the simulation and analytical results confirms the correctness of the presented analysis.

I. INTRODUCTION

THE commercial deployment of the 5G wireless communications network has already begun in mid-2019 in many countries. The first phase of 5G mobile communications is expected to be operating in the 3.6 GHz range. However, the amount of spectrum in the sub-GHz and below 6 GHz range, which will support many crucial applications in 5G, is very congested [1]. With the advent of many new wireless communication applications and services, the number of devices/users accessing the wireless spectrum is increasing very rapidly, resulting in the problem of *spectrum scarcity*. On the other hand, it is well-known that the 3.5 GHz band (along with some ISM and mmWave bands) are currently under-utilized, and therefore *spectrum sharing* is considered as a potential solution to enhance the spectrum usage efficiency [2]–[4]. On the other hand, NOMA has also gained tremendous attention as a potential multiple access technique for the next-generation

mobile communications network, as it can provide *massive connectivity* and can also enhance the spectral efficiency [5]–[7].

In general, spectrum sharing between a licensed/primary network and an unlicensed/secondary network can be accomplished in three ways: *underlay*, *interweave* and *overlay* [2]. In the case of underlay spectrum sharing, the ST transmits simultaneously with the primary-user transmitter (PT) using the band of frequencies originally owned by the primary network, in such a manner that the interference inflicted by the secondary network on the primary network is below a tolerance limit. In interweave spectrum sharing, a cognitive engine first determines the spectrum bands for which the usage license is owned by a primary network and the secondary network uses those licensed bands when primary activity is not detected in those bands. Determination of these *spectrum holes* by the cognitive engine is termed as *spectrum sensing*. In the case of overlay spectrum sharing, the secondary user transmits simultaneously with the primary user, but compensates for the interference caused on the primary network by relaying a part of the primary user's message to the intended receiver(s). The fusion of NOMA and spectrum sharing has gained particular attention in the past few years, as it has the potential to provide massive connectivity and to further enhance the spectrum utilization efficiency in beyond-5G systems.

For the case of overlay spectrum sharing, many notable works analyzing the achievable rate, outage probability, throughput and optimal power allocation have been presented for different NOMA systems such as multi-user secondary network, energy harvesting STs, relay-based cooperative systems and hybrid satellite-terrestrial networks [8]–[12].

On the other hand, there has also been particular research attention given to underlay spectrum sharing NOMA systems. Different cooperative and non-cooperative NOMA-based spectrum sharing architectures were proposed in [13], including underlay, overlay and cognitive radio (CR) inspired NOMA. It was shown in [13] that NOMA-based spectrum sharing outperforms its OMA-based counterpart in terms of outage probability. The outage probability analysis of a NOMA-based underlay spectrum sharing system was presented in [14], where the power transmitted by the ST was constrained by a peak tolerable interference power at PRs as well as a peak power budget at the ST. In [15], the outage performance analysis of a relay-based underlay spectrum sharing NOMA system, consisting of one ST, one detect-and-forward relay, one PR and two secondary receivers (SRs), was presented, where the power transmitted from the ST was constrained by a peak interference constraint at the PR as well as a peak power

V. Kumar and M. F. Flanagan are with School of Electrical and Electronic Engineering, University College Dublin, Dublin D04 V1W8, Ireland (e-mail: vaibhav.kumar@ieee.org, mark.flanagan@ieee.org).

Z. Ding is with School of Electrical and Electronic Engineering, The University of Manchester, Manchester M13 9PL, U.K. (e-mail: zhiguo.ding@manchester.ac.uk).

This work was supported by Science Foundation Ireland (SFI) through Grant 17/US/3445 and co-funded through the European Regional Development Fund under Grant 13/RC/2077.

budget at the ST. However, in [15], it was assumed that the transmission from the relay does not cause any interference at the PR (due to a large separation between them), and the signal received at the relay and the two SRs were also assumed to be free from any interference from the primary network. The analysis of outage probability for a relay-based spectrum sharing NOMA system considering the relay-to-PR interference was presented in [16]. The outage probability and throughput analysis of an underlay spectrum sharing hybrid OMA/NOMA system consisting of a PT, a PR, an ST and two SRs was presented in [17], where the authors considered both primary-to-secondary and secondary-to-primary interference. The power transmitted from the ST was constrained by a peak interference constraint at the PR as well as a peak power budget constraint at the ST. However, it is noteworthy that the closed-form expressions for the system throughput (or the average achievable sum-rate) was not derived in [17]. The performance analysis in terms of average achievable sum-rate, outage probability and asymptotic behavior (of outage probability) of a NOMA-based cooperative relaying system in an underlay spectrum sharing scenario, considering only the peak interference constraint, was presented in [18] (here the authors assumed that the ST and relay do not have any power budget constraints). In [19], the analysis of the outage probability for an underlay spectrum-sharing-inspired amplify-and-forward relay-based two-user downlink NOMA system was presented, where the power transmitted from the ST was assumed to be constrained by a peak power budget at the ST as well as a peak interference constraint at the PR.

In summary, for the case of NOMA-based underlay spectrum sharing, most existing research deals only with the outage probability analysis (as in [14]–[17], [19]) or considers only the peak interference constraint at the PR (as in [18]). It is also noteworthy that only single-antenna receivers were considered in [14]–[17], [19]. Also note that perfect instantaneous CSI regarding the ST-PR link(s) was assumed to be available at the ST in [14], [15], [18] and [19], whereas imperfect instantaneous CSI regarding the ST-PR link was assumed to be available at the ST in [16] and [17]. Motivated by this, in this paper, we present the average achievable sum-rate and outage probability analysis of a two-user downlink NOMA system in underlay spectrum sharing (over Rayleigh fading wireless channels) where both of the (secondary) users are assumed to be equipped with multiple antennas. We also consider that only statistical channel state information (CSI) is available at the ST regarding the links between the ST and the users¹, whereas, for the case of the link between the ST and PR, we consider different scenarios, as explained in Table I. Hereafter, we will refer to the CSI of the ST-PR link as the interference-link CSI

(IL-CSI).

The main contributions of this paper are summarized as follows:

- We derive closed-form expressions for the average achievable sum-rate and outage probability for the spectrum sharing NOMA system for all the five cases shown in Table I.
- For the special case where the secondary users are each equipped with a single receive antenna, we derive an explicit analytical expression for the optimal power allocation coefficient that minimizes the outage probability of the spectrum sharing NOMA system (except for the case of PowIntICSI). For the general case, where the users are equipped with more than one receive antenna, the value of optimal power allocation coefficient is obtained numerically.
- By comparing the performance of the spectrum sharing NOMA system with the corresponding OMA system, we show that the NOMA system outperforms its OMA-based counterpart by achieving lower outage probability and higher achievable rate. More interestingly, we show a performance comparison among different system configurations of the spectrum sharing NOMA system (as described in Table I) to show the effect of loss of information (in terms of CSI) on the overall system performance.
- For the case of NOMA systems, our results confirm that when the value of the peak tolerable interference at the PR is large and the SRs are equipped with a large number of antennas, the difference between the performance of IntICSI and IntSCSI is negligible in terms of outage probability, whereas the performance difference is significant in terms of achievable sum-rate. A similar trend is observed in the *interference-constrained regime* (to be explained later) when the performance (as regards outage probability as well as achievable sum-rate) of PowIntICSI, PowIntSCSI and PowIntOneBit are compared. Interestingly, the results also confirm that for the case of PowIntOneBit NOMA, a higher power budget at the ST results in an inferior performance (both in terms of outage probability and achievable sum-rate) in the interference-constrained regime.

The achievable rate analysis of an underlay spectrum sharing OMA system (with a single downlink secondary user) considering peak or average interference constraint and unlimited or limited power-budget constraint, was presented in [20]. The authors demonstrated the effect of different levels of IL-CSI on the achievable rate of the secondary user. The main difference between the work presented in [20] and that of this paper is that we consider a (downlink) multiple access system, whereas in [20] only a single downlink user was considered. Also, in the work presented in [20], the authors considered a single-antenna-assisted downlink user, while here we consider multi-antenna-assisted downlink users. It is also important to note that along with the achievable rate analysis, we also present the outage probability analysis of the spectrum sharing system, which was not presented in [20].

¹For the case of a spectrum sharing system, the ST needs to coordinate with the primary network in order to acquire CSI for the ST-PR link(s). This results in extra overhead at the ST as compared to the traditional (licensed) systems. Since for the secondary channels (i.e., the channels between the ST and the NOMA users), acquiring statistical CSI requires a smaller overhead as compared to that for instantaneous CSI, we have considered the former in order to reduce the communication overhead at the ST. However, it can be shown that it is straightforward to extend the analysis presented in this paper to the case when instantaneous CSI is available at the ST regarding the secondary channels.

TABLE I
DETAILS OF THE DIFFERENT SYSTEM CONFIGURATIONS ANALYZED IN THIS WORK.

Case	Power budget at ST	IL-CSI at ST	Insights (for NOMA)
IntICSI	Unlimited	Instantaneous	The difference between the outage probability of IntICSI and IntSCSI becomes negligible for a large number of antennas and a large value of the peak tolerable interference. The rate of decay of the outage probability depends on the minimum number of antennas at the NOMA users. However, a significant difference can be noted between the achievable sum-rate of the two systems, even for a large number of antennas and/or for a large value of interference. Using asymptotic rate analysis, we show that there is no benefit (in terms of achievable rate) from having multiple antennas at the far user.
IntSCSI	Unlimited	Statistical	
PowIntICSI	Limited	Instantaneous	The system experiences an outage floor, as well as a rate saturation, in the power-constrained regime. A higher power budget is advantageous for these systems in the power-constrained regime. However, no significant benefit is observed from a higher power budget in the interference constrained regime for PowIntICSI and PowIntSCSI system, whereas for the case of the PowIntOneBit system, a higher power budget results in an inferior performance in the interference constrained regime. The benefit of using a large number of antennas is significant in both the regimes.
PowIntSCSI	Limited	Statistical	
PowIntOneBit	Limited	No CSI	

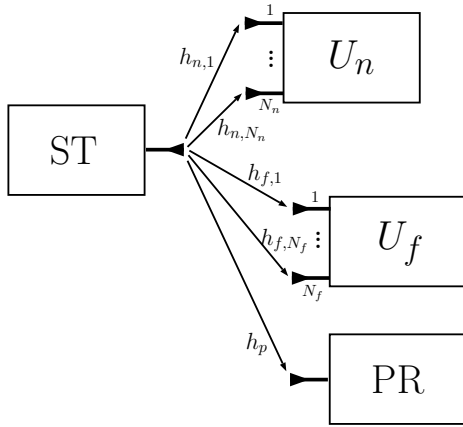


Fig. 1. System model for underlay spectrum sharing. Here U_n and U_f are the secondary-user receivers.

II. SYSTEM MODEL

Consider the system shown in Fig. 1, consisting of a secondary-user transmitter ST, a primary-user receiver PR and two secondary-user receivers U_n and U_f . It is assumed that the ST and PR are each equipped with a single antenna, whereas U_n and U_f are equipped with $N_n (\geq 1)$ and $N_f (\geq 1)$ antennas, respectively. The channel fading coefficient between the ST and the PR is denoted by h_p , whereas that between the ST and the i -th antenna of U_n , and the ST and the j -th antenna of U_f are denoted by $h_{n,i}$ and $h_{f,j}$, respectively, where $i \in \{1, 2, \dots, N_n\}$ and $j \in \{1, 2, \dots, N_f\}$. We assume that $h_p \sim \mathcal{CN}(0, \Omega_p = d_p^{-\alpha})$, $h_{n,i} \sim \mathcal{CN}(0, \Omega_n = d_n^{-\alpha})$ and $h_{f,j} \sim \mathcal{CN}(0, \Omega_f = d_f^{-\alpha})$ where d_p , d_n and d_f denote the distance between the ST and PR, ST and U_n , and ST and U_f , respectively, and α denotes the path-loss exponent. Throughout this paper, we assume that the ST has statistical channel state information (CSI) regarding the links between the ST and U_n , and ST and U_f , i.e., the knowledge of Ω_n , Ω_f and the corresponding distribution of these links, whereas the availability of the CSI regarding the ST-PR link, i.e., the IL-CSI for different scenarios, is given in Table I. It is also assumed that $d_n < d_f < d_p$, and we therefore refer to U_n

and U_f as the near and far users respectively. We consider the scenario where the secondary network (consisting of ST, U_n and U_f) is deployed outside the coverage of the primary-user transmitter, and therefore, we do not consider the interference at U_n and U_f caused by the primary-user transmitter.

In the case of NOMA, the ST broadcasts a power-division multiplexed symbol

$$\sqrt{a_n P_t(g_p)} x_n + \sqrt{a_f P_t(g_p)} x_f,$$

where x_n and x_f are the unit-energy symbols intended for users U_n and U_f , respectively, a_n and a_f are the power allocation coefficients for users U_n and U_f , respectively (we assume that $a_n < a_f$ and $a_n + a_f = 1$), $g_p \triangleq |h_p|^2$, and $P_t(g_p)$ is the total power transmitted from the ST. In general, $P_t(g_p)$ is a one-to-one mapping from the channel gain g_p to the set of non-negative real numbers \mathbb{R}_+ . Note that the notation $P_t(g_p)$ indicates that the ST has the perfect knowledge of the channel gain g_p ; in the sequel, when we consider the case where the ST has no knowledge or only statistical knowledge of the channel gain g_p , we will denote the power transmitted from the ST simply by P_t .

After receiving the signals, the user $U_u, u \in \{n, f\}$ first combines the signals using maximal-ratio combining (MRC), and therefore, the channel gain between the ST and U_u is given by $g_u \triangleq \mathbf{h}_u^H \mathbf{h}_u$, where $\mathbf{h}_u = [h_{u,1} \ h_{u,2} \ \dots \ h_{u,N_u}]^T \in \mathbb{C}^{N_u \times 1}$. The near user U_n first decodes x_f by considering the inter-user interference due to the presence of x_n in the received signal as additional noise. It then applies successive interference cancellation (SIC) to remove x_f from the received signal and then decodes its intended symbol x_n . On the other hand, the far user U_f decodes x_f directly considering the interference due to x_n as additional noise. Assuming the noise contributions at all receiver nodes to be distributed as $\mathcal{CN}(0, 1)$, the instantaneous signal-to-interference-plus-noise ratio (SINR) and instantaneous signal-to-noise ratio (SNR) at U_n to decode x_f and x_n are, respectively, given by

$$\gamma_n^{(f)} = \frac{a_f g_n P_t(g_p)}{a_n g_n P_t(g_p) + 1}, \quad \gamma_n^{(n)} = a_n g_n P_t(g_p).$$

Similarly, the instantaneous SINR at U_f to decode x_f is given by

$$\gamma_f^{(f)} = \frac{a_f g_f P_t(g_p)}{a_n g_f P_t(g_p) + 1}.$$

Since symbol x_n needs to be decoded only by U_n , the instantaneous achievable rate for U_n is given by

$$\log_2 [1 + \gamma_n^{(n)}] = \log_2 [1 + a_n g_p P_t(g_p)].$$

On the other hand, since x_f needs to be decoded by both users, the instantaneous achievable rate for U_f is given by

$$\begin{aligned} & \min \left\{ \log_2 [1 + \gamma_n^{(f)}], \log_2 [1 + \gamma_f^{(f)}] \right\} \\ &= \log_2 \left[1 + \frac{a_f g_{\min} P_t(g_p)}{a_n g_{\min} P_t(g_p) + 1} \right], \end{aligned}$$

where $g_{\min} \triangleq \min\{g_n, g_f\}$.

In contrast to this, for the case of OMA, the ST transmits $\sqrt{P_t(g_p)}x_n$ and $\sqrt{P_t(g_p)}x_f$ to U_n and U_f , respectively, in two orthogonal time slots. Therefore, the instantaneous SNR at U_n and U_f to decode the intended symbol is, respectively, given by

$$\hat{\gamma}_n = g_n P_t(g_p), \quad \hat{\gamma}_f = g_f P_t(g_p).$$

Throughout this paper, $f_{\mathcal{X}}(\cdot)$, $F_{\mathcal{X}}(\cdot)$, $F_{\mathcal{X}}^{-1}(\cdot)$ and $\mathcal{F}_{\mathcal{X}}(\cdot)$ denote the probability density function (PDF), cumulative distribution function (CDF), inverse distribution function (IDF), and complementary CDF (CCDF) of the random variable \mathcal{X} , respectively.

Next, we will present the achievable rate, outage probability and optimal power allocation for the spectrum sharing system.

III. SECONDARY PERFORMANCE FOR INTICSI

In this section, we assume that the ST has perfect instantaneous IL-CSI, and adapts its transmission power such that the instantaneous interference caused by the ST at the PR is less than a predefined threshold value I . In addition, we do not consider any power budget limit for the ST. Such a scenario is relevant when the ST is one with unlimited power, such as a base station.

A. Average achievable sum-rate

The average achievable sum-rate for the NOMA system is given by

$$\begin{aligned} C_{\text{sum}} &= \max_{P_t(g_p) \geq 0} \mathbb{E}_{g_p, g_n, g_f} \left\{ \log_2 [1 + a_n g_n P_t(g_p)] \right. \\ &\quad \left. + \log_2 \left[1 + \frac{a_f g_{\min} P_t(g_p)}{a_n g_{\min} P_t(g_p) + 1} \right] \right\}, \quad (1) \end{aligned}$$

$$\text{s.t. } g_p P_t(g_p) \leq I. \quad (2)$$

The optimal transmit power $P_t^*(g_p)$ that maximizes C_{sum} in (1) is given by I/g_p . Therefore, the expression for the average achievable sum-rate is given by

$$C_{\text{sum}} = \mathbb{E}_{X_n} \{ \log_2 (1 + a_n I X_n) \}$$

$$+ \mathbb{E}_{X_{\min}} \{ \log_2 (1 + I X_{\min}) \} - \mathbb{E}_{X_{\min}} \{ \log_2 (1 + a_n I X_{\min}) \}, \quad (3)$$

where $X_n \triangleq g_n/g_p$ and $X_{\min} \triangleq g_{\min}/g_p$.

Theorem 1. For the case of IntICSI, the average achievable sum-rate for the NOMA system is given by (4), shown on the next page, where $\Omega \triangleq \Omega_n \Omega_f / (\Omega_n + \Omega_f)$ and $G(\cdot)$ denotes Meijer's G-function.

Proof. See Appendix A. ■

On the other hand, for the case of OMA, the average achievable sum-rate is given by

$$\mathcal{C}_{\text{sum}} = 0.5 \sum_{u \in \{n, f\}} \mathbb{E}_{X_u} \{ \log_2 (1 + I X_u) \}, \quad (5)$$

where $X_u \triangleq g_u/g_p$. Note that for a fair comparison, in (5) the peak tolerable interference value I is the same as considered for the NOMA systems. Also, note that one transmission cycle in NOMA takes a single time slot, whereas for OMA (time-division multiplexed system), one transmission cycle takes two time slots; therefore, a factor of 0.5 is included in (5) for fair comparison between NOMA and OMA systems. We do not provide a closed-form analysis for the case of OMA, as the focus of this paper is on the NOMA-based system. For the purpose of comparison, we will evaluate the performance of the OMA-based system numerically.

Asymptotic analysis: For the limiting case where $I \rightarrow \infty$, it is straightforward to observe that the average achievable rate for U_f converges to $\log_2(1 + a_f/a_n) = \log_2(1/a_n)$. Therefore, the average achievable sum-rate for NOMA can be approximated by

$$\begin{aligned} C_{\text{sum}} &\approx \mathbb{E}_{X_n} \{ \log_2 (a_n I X_n) \} + \log_2 \left(\frac{1}{a_n} \right) \\ &= \frac{N_n}{\Omega_n^{N_n} \Omega_p} \int_0^\infty x^{N_n-1} \log_2 (a_n I x) \left(\frac{x}{\Omega_n} + \frac{1}{\Omega_p} \right)^{-(N_n+1)} dx \\ &\quad + \log_2 \left(\frac{1}{a_n} \right) \\ &= \log_2(e) \left[\mathfrak{E} + \ln \left(\frac{a_n \Omega_n I}{\Omega_p} \right) + \mathfrak{D}(N_n) + \ln \left(\frac{1}{a_n} \right) \right], \quad (6) \end{aligned}$$

where \mathfrak{E} is the Euler-Mascheroni constant and $\mathfrak{D}(\cdot)$ is the digamma function. This leads to a couple of important observations:

- For large I , there is no benefit (in terms of achievable rate) from having multiple antennas at the far user.
- For large I , when the number of antennas at the near user is increased from (say) $N_n^{(1)}$ to $N_n^{(2)}$, the gain in the near user's achievable rate is quantified by $\log_2(e) \left[\mathfrak{D}(N_n^{(2)}) - \mathfrak{D}(N_n^{(1)}) \right]$. This is also equal to the gain in average achievable sum-rate for the NOMA system.

Next we present the analysis of the outage probability for both NOMA and OMA systems.

$$\begin{aligned}
C_{\text{sum}} = & \frac{1}{\ln 2} \left[\frac{1}{\Gamma(N_n)} \left(\frac{\Omega_p}{\Omega_n a_n I} \right)^{N_n} G_{3,3}^{3,2} \left(\frac{\Omega_p}{\Omega_n a_n I} \middle| \begin{matrix} -N_n, -N_n, 1-N_n \\ 0, -N_n, -N_n \end{matrix} \right) + \sum_{k=0}^{N_f-1} \frac{\Omega_p^{N_n+k}}{\Gamma(N_n) k! \Omega_n^{N_n} \Omega_f^k I^{N_n+k}} \right. \\
& \times \left\{ G_{3,3}^{3,2} \left(\frac{\Omega_p}{\Omega I} \middle| \begin{matrix} -N_n-k, -N_n-k, 1-N_n-k \\ 0, -N_n-k, -N_n-k \end{matrix} \right) - \frac{1}{a_n^{N_n+k}} G_{3,3}^{3,2} \left(\frac{\Omega_p}{\Omega a_n I} \middle| \begin{matrix} -N_n-k, -N_n-k, 1-N_n-k \\ 0, -N_n-k, -N_n-k \end{matrix} \right) \right\} + \sum_{l=0}^{N_n-1} \frac{\Omega_p^{N_f+l}}{\Gamma(N_f) l!} \\
& \times \frac{1}{\Omega_f^{N_f} \Omega_n^l I^{N_f+l}} \left\{ G_{3,3}^{3,2} \left(\frac{\Omega_p}{\Omega I} \middle| \begin{matrix} -N_f-l, -N_f-l, 1-N_f-l \\ 0, -N_f-l, -N_f-l \end{matrix} \right) - \frac{1}{a_n^{N_f+l}} G_{3,3}^{3,2} \left(\frac{\Omega_p}{\Omega a_n I} \middle| \begin{matrix} -N_f-l, -N_f-l, 1-N_f-l \\ 0, -N_f-l, -N_f-l \end{matrix} \right) \right\} \Bigg]. \quad (4)
\end{aligned}$$

B. Outage probability

We assume that the target data rates for users U_n and U_f are the same, and are denoted by r_{target} . Therefore, for the case of NOMA, the outage threshold is defined as $\theta \triangleq 2^{r_{\text{target}}} - 1$.

Theorem 2. *For the case of IntICSI, the outage probability for the NOMA system is given by*

$$\mathbb{P}_{\text{out}} = 1 - \prod_{u \in \{n, f\}} \left[1 - \left(\frac{\Omega_p \xi_u}{\Omega_u I + \Omega_p \xi_u} \right)^{N_u} \right], \quad (7)$$

where $\xi_n \triangleq \theta \max \left\{ \frac{1}{a_f - a_n \theta}, \frac{1}{a_n} \right\}$ and $\xi_f \triangleq \frac{\theta}{a_f - a_n \theta}$.

Proof. See Appendix B. ■

It is noteworthy that the term $a_f - a_n \theta$ in the denominator of ξ_f indicates that we require $a_f > a_n \theta$, i.e., $a_n < 1/(1 + \theta)$, otherwise both U_n and U_f will fail to decode x_f and the outage probability of the system will always be equal to 1. A similar phenomenon was observed in [18] and [21].

On the other hand, for the case of OMA, the outage threshold is defined as $\Theta \triangleq 2^{2r_{\text{target}}} - 1$ and the outage probability is given by

$$\mathcal{P}_{\text{out}} = 1 - \prod_{u \in \{n, f\}} \Pr(I X_u \geq \Theta). \quad (8)$$

Here we do not provide a closed-form expression for the outage probability for the case of OMA, but we will rather evaluate via simulation for the purpose of comparison.

Asymptotic analysis: For the limiting case where $I \rightarrow \infty$, it can be shown using the binomial expansion that

$$\begin{aligned}
\mathbb{P}_{\text{out}} = & \sum_{k=0}^{\infty} (-1)^k \binom{N_f + k - 1}{k} \Psi_f^{N_f+k} I^{-(N_f+k)} + \sum_{l=0}^{\infty} (-1)^l \\
& \times \binom{N_n + l - 1}{l} \Psi_n^{N_n+l} I^{-(N_n+l)} - \sum_{k=0}^{N_f} \sum_{l=0}^{N_n} (-1)^{k+l} \\
& \times \binom{N_f + k - 1}{k} \binom{N_n + l - 1}{l} \Psi_f^{N_f+k} \Psi_n^{N_n+l} I^{-(N_f+N_n+k+l)},
\end{aligned}$$

where $\Psi_u \triangleq \Omega_p \xi_u / \Omega_u$. Using the preceding expression, it is straightforward to conclude that \mathbb{P}_{out} decays as $I^{-\min\{N_n, N_f\}}$ for large values of I .

C. Optimal power allocation

In this subsection, we attempt to find a closed-form expression for the optimal a_n , denoted by a_n^* , that minimizes the outage probability of the spectrum sharing NOMA system. By differentiating (7), it can be observed that a closed-form expression for a_n^* is not possible in general. However, in the following theorem we show that this is possible in the special case $N_n = N_f = 1$.

Theorem 3. *For the case of IntICSI with $N_n = N_f = 1$, a_n^* is given by*

$$\begin{aligned}
a_n^* = & \frac{I \Omega_f + \Omega_p \theta}{I \{(1 + \theta) \Omega_f - \Omega_n\}} \\
& - \frac{\sqrt{(1 + \theta)(I \Omega_f + \Omega_p \theta) \{I \Omega_n + \Omega_p \theta (1 + \theta)\}}}{I(1 + \theta) \{(1 + \theta) \Omega_f - \Omega_n\}}. \quad (9)
\end{aligned}$$

Proof. See Appendix C. ■

With simple algebraic manipulation, it can be shown that for the case when $N_n = N_f = 1$, the value of a_n^* decreases with an increase in the value of I . For the case when $N_n > 1$ and $N_f > 1$, we find the optimal value of a_n numerically.

IV. SECONDARY PERFORMANCE FOR INTSCSI

In a practical system, it is often not possible to obtain instantaneous CSI at the transmitter side. Motivated by this issue, we consider the scenario where the ST has only the statistical CSI regarding the ST-PR link, i.e., only the information regarding Ω_p and the distribution of h_p is available at the ST (along with the statistical CSI of the ST- U_u links). In this case, the quality-of-service (QoS) at the PR is protected through a statistical constraint which states that the probability that the interference caused by the ST to the PR is above the interference threshold I should be lower than a preset threshold δ . Denoting the power transmitted from ST by P_t , we have

$$\begin{aligned}
& \Pr(g_p P_t > I) \leq \delta \\
& \implies 1 - F_{g_p}(I/P_t) \leq \delta \implies P_t \leq \frac{I}{F_{g_p}^{-1}(1 - \delta)}. \quad (10)
\end{aligned}$$

Given that g_p is an exponentially distributed random variable with mean value given by Ω_p , the IDF of g_p is given by $F_{g_p}^{-1}(x) = -\Omega_p \ln(1 - x)$. Substituting the expression for $F_{g_p}^{-1}(\cdot)$ into (10), the optimal transmit power to maximize the average achievable sum-rate is given by

$$P_t^* = -I/(\Omega_p \ln \delta). \quad (11)$$

Next, we will provide analytical expressions for the average achievable sum-rate, outage probability and optimal power allocation in spectrum sharing NOMA system for the IntSCSI case.

A. Average achievable sum-rate

The expression for the average achievable sum-rate in NOMA is be given by

$$C_{\text{sum}} = \mathbb{E}_{g_n} \{ \log_2(1 + a_n g_n P_t^*) \} + \mathbb{E}_{g_{\min}} \{ \log_2(1 + g_{\min} P_t^*) \} - \mathbb{E}_{g_{\min}} \{ \log_2(1 + a_n g_{\min} P_t^*) \}. \quad (12)$$

Theorem 4. For the case of IntSCSI, the average achievable sum-rate for NOMA is given by (13), shown on the next page.

Proof. See Appendix D. ■

On the other hand, for the case of OMA, the expression for the average achievable sum-rate is given by

$$\mathcal{C}_{\text{sum}} = 0.5 \sum_{u \in \{n, f\}} \mathbb{E}_{g_u} \left\{ \log_2 \left(1 - \frac{g_u I}{\Omega_p \ln \delta} \right) \right\}. \quad (14)$$

Asymptotic analysis: Similar to the IntICSI case, for large I , the average achievable sum-rate for NOMA can be approximated by

$$\begin{aligned} C_{\text{sum}} &= \mathbb{E}_{g_n} \left\{ \log_2 \left(a_n g_n \frac{I}{\Omega_p (-\ln \delta)} \right) \right\} + \log_2 \left(\frac{1}{a_n} \right) \\ &= \frac{1}{\Gamma(N_n) \Omega_n^{N_n}} \int_0^\infty \log_2 \left(\frac{a_n I}{\Omega_p (-\ln \delta)} x \right) x^{N_n-1} \\ &\quad \times \exp \left(\frac{-x}{\Omega_n} \right) dx + \log_2 \left(\frac{1}{a_n} \right) \\ &= \log_2(e) \left[\ln \left(\frac{a_n \Omega_n I}{\Omega_p (-\ln \delta)} \right) + \mathfrak{D}(N_n) + \ln \left(\frac{1}{a_n} \right) \right]. \end{aligned} \quad (15)$$

Similar to the case of IntICSI, for large I , there is no benefit (in terms of achievable rate) from having multiple antennas at the far user. Also, for large I , when the number of antennas at the near user is increased from $N_n^{(1)}$ to $N_n^{(2)}$, the gain in average achievable sum-rate can be quantified by $\log_2(e) [\mathfrak{D}(N_n^{(2)}) - \mathfrak{D}(N_n^{(1)})]$, which is the same as for the case of IntICSI.

B. Outage probability

Following similar arguments as used in Section III-B, the outage probability for NOMA is given by

$$\begin{aligned} \mathbb{P}_{\text{out}} &= 1 - \Pr \left(\frac{a_f P_t^* g_n}{1 + a_n P_t^* g_n} \geq \theta, a_n P_t^* g_n \geq \theta \right) \\ &\quad \times \Pr \left(\frac{a_f P_t^* g_f}{1 + a_n P_t^* g_f} \geq \theta \right) \\ &= 1 - \Pr \left(g_n \geq \frac{\theta}{P_t^*} \max \left\{ \frac{1}{a_f - a_n \theta}, \frac{1}{a_n} \right\} \right) \\ &\quad \times \Pr \left(g_f \geq \frac{\theta}{P_t^* (a_f - a_n \theta)} \right) \end{aligned}$$

$$\begin{aligned} &= 1 - \prod_{u \in \{n, f\}} \mathcal{F}_{g_u} \left(\frac{\xi_u}{P_t^*} \right) \\ &= 1 - \prod_{u \in \{n, f\}} \frac{1}{\Gamma(N_u) \Omega_u^{N_u}} \int_{\xi_u / P_t^*}^\infty x^{N_u-1} \exp \left(\frac{-x}{\Omega_u} \right) dx \\ &= 1 - \prod_{u \in \{n, f\}} \frac{\Gamma[N_u, \xi_u / (\Omega_u P_t^*)]}{\Gamma(N_u)}, \end{aligned} \quad (16)$$

where the integral above is solved using [22, eqn. (3.381-3), p. 346] and $\Gamma[\cdot, \cdot]$ denotes the upper-incomplete Gamma function.

On the other hand, for the case of OMA, the outage probability is given by

$$\mathcal{P}_{\text{out}} = 1 - \prod_{u \in \{n, f\}} \Pr(P_t^* g_u \geq \Theta). \quad (17)$$

Asymptotic analysis: Using [23, eqn. (8.7.2), p. 178], it can be shown that

$$\begin{aligned} \mathbb{P}_{\text{out}} &= \frac{1}{\Gamma(N_f)} \sum_{k=0}^\infty \frac{(-1)^k \Upsilon_f^{N_f+k}}{k! (N_f+k)} I^{-(N_f+k)} + \frac{1}{\Gamma(N_n)} \\ &\quad \times \sum_{l=0}^\infty \frac{(-1)^l \Upsilon_n^{N_n+l}}{l! (N_n+l)} I^{-(N_n+l)} - \frac{1}{\Gamma(N_f) \Gamma(N_n)} \\ &\quad \times \sum_{k=0}^\infty \sum_{l=0}^\infty \frac{(-1)^{k+l} \Upsilon_f^{N_f+k} \Upsilon_n^{N_n+l}}{k! l! (N_f+k)(N_n+l)} I^{-(N_f+N_n+k+l)}, \end{aligned}$$

where $\Upsilon_u \triangleq -\xi_u \Omega_p \ln \delta / \Omega_u$. From the preceding equation, it is straightforward to conclude that \mathbb{P}_{out} decays as $I^{-\min\{N_n, N_f\}}$ for large values of I .

C. Optimal power allocation

Theorem 5. For the case of IntSCSI with $N_n = N_f = 1$, a_n^* is given by

$$a_n^* = \frac{\Omega_f}{(1+\theta)\Omega_f - \Omega_n} - \frac{\sqrt{\Omega_n \Omega_f (1+\theta)}}{(1+\theta) \{ (1+\theta)\Omega_f - \Omega_n \}}. \quad (18)$$

Proof. See Appendix E. ■

It is important to note that in this case, the optimal value of a_n does not depends on I or Ω_p .

Next, we present the analysis for the spectrum sharing system where a power budget constraint also exists at the ST, along with a peak interference constraint at the PR.

V. SECONDARY PERFORMANCE FOR POWINTICSI

For the case when the ST is a battery-operated device, the power transmitted from the ST is often constrained by a peak power budget at the ST. Therefore, in this section, we analyze the performance of the spectrum sharing system where the power transmitted from the ST is constrained by the peak interference caused at the PR as well as a peak power budget at the ST.

$$\begin{aligned}
C_{\text{sum}} = & \frac{1}{\ln 2} \left[\frac{1}{\Gamma(N_n)\Omega_n^{N_n}(a_n P_t^*)^{N_n}} G_{2,3}^{3,1} \left(\frac{1}{\Omega_n a_n P_t^*} \middle| \begin{matrix} -N_n, 1-N_n \\ 0, -N_n, -N_n \end{matrix} \right) + \frac{1}{\Gamma(N_n)\Omega_n^{N_n}} \sum_{k=0}^{N_f-1} \frac{1}{k! \Omega_f^k (P_t^*)^{N_n+k}} \right. \\
& \times \left\{ G_{2,3}^{3,1} \left(\frac{1}{\Omega P_t^*} \middle| \begin{matrix} -N_n-k, 1-N_n-k \\ 0, -N_n-k, -N_n-k \end{matrix} \right) - \frac{1}{a_n^{N_n+k}} G_{2,3}^{3,1} \left(\frac{1}{\Omega a_n P_t^*} \middle| \begin{matrix} -N_n-k, 1-N_n-k \\ 0, -N_n-k, -N_n-k \end{matrix} \right) \right\} + \frac{1}{\Gamma(N_f)\Omega_f^{N_f}} \\
& \times \sum_{l=0}^{N_n-1} \frac{1}{l! \Omega_n^l (P_t^*)^{N_f+l}} \left\{ G_{2,3}^{3,1} \left(\frac{1}{\Omega P_t^*} \middle| \begin{matrix} -N_f-l, 1-N_f-l \\ 0, -N_f-l, -N_f-l \end{matrix} \right) - \frac{1}{a_n^{N_f+l}} G_{2,3}^{3,1} \left(\frac{1}{\Omega a_n P_t^*} \middle| \begin{matrix} -N_f-l, 1-N_f-l \\ 0, -N_f-l, -N_f-l \end{matrix} \right) \right\} \Big]. \quad (13)
\end{aligned}$$

A. Average achievable sum-rate

The average achievable sum-rate for the NOMA system is given by

$$\begin{aligned}
C_{\text{sum}} = & \max_{P_t(g_p) \geq 0} \mathbb{E}_{g_p, g_n, g_f} \left\{ \log_2[1 + a_n g_n P_t(g_p)] \right. \\
& \left. + \log_2 \left[1 + \frac{a_f g_{\min} P_t(g_p)}{a_n g_{\min} P_t(g_p) + 1} \right] \right\}, \quad (19)
\end{aligned}$$

$$\text{s.t. } g_p P_t(g_p) \leq I, \quad (20)$$

$$P_t(g_p) \leq P_{\text{peak}}, \quad (21)$$

where P_{peak} denotes the peak power budget at the ST. Therefore, the optimal power to maximize the average achievable sum-rate in NOMA is given by

$$P_t^*(g_p) = \min \left\{ P_{\text{peak}}, \frac{I}{g_p} \right\} = \begin{cases} P_{\text{peak}}, & \text{if } g_p \leq \frac{I}{P_{\text{peak}}} \\ \frac{I}{g_p}, & \text{otherwise.} \end{cases} \quad (22)$$

Therefore, using (19)-(22), the expression for the average achievable sum-rate for NOMA is given by

$$\begin{aligned}
C_{\text{sum}} = & \mathbb{E}_{g_p, g_n} \{ \log_2[1 + a_n g_n P_t^*(g_p)] \} \\
& + \mathbb{E}_{g_p, g_{\min}} \{ \log_2[1 + P_t^*(g_p) g_{\min}] \} \\
& - \mathbb{E}_{g_p, g_{\min}} \{ \log_2[1 + a_n P_t^*(g_p) g_{\min}] \}, \quad (23)
\end{aligned}$$

where $P_t^*(g_p)$ is given by (22). It can be shown that in general, it is very difficult (if not impossible) to find an analytical expression for (23). Therefore, we present the analytical expression for the special case where $N_n = N_f = 1$.

Theorem 6. For the case of PowIntICSI with $N_n = N_f = 1$, the average achievable sum-rate for NOMA is given by

$$C_{\text{sum}} = \frac{1}{\ln 2} [T(a_n \Omega_n) + T(\Omega) - T(a_n \Omega)], \quad (24)$$

where $T(x)$ is given in (25) (shown on the next page) in which $\text{Shi}(\cdot)$ and $\text{Chi}(\cdot)$ denote the hyperbolic sine and hyperbolic cosine integrals, respectively.

Proof. See Appendix F. ■

On the other hand, the corresponding average achievable sum-rate for OMA is given by

$$\mathcal{C}_{\text{sum}} = 0.5 \sum_{u \in \{n, f\}} \mathbb{E}_{g_u} \{ \log_2(1 + g_u P_t^*(g_p)) \}. \quad (26)$$

Asymptotic analysis: For the limiting case when $I \rightarrow \infty$, we give an analytical expression for the more general case where $N_n \geq 1$ and $N_f \geq 1$. In this case, for a finite value of P_{peak} , we have

$$\lim_{I \rightarrow \infty} P_t^*(g_p) = \lim_{I \rightarrow \infty} \min \left\{ P_{\text{peak}}, \frac{I}{g_p} \right\} = P_{\text{peak}}.$$

Therefore, the asymptotic expression for the average achievable sum-rate is given by

$$\begin{aligned}
C_{\text{sum}} = & \mathbb{E}_{g_n} \{ \log_2[1 + a_n g_n P_{\text{peak}}] \} \\
& + \mathbb{E}_{g_{\min}} \{ \log_2[1 + g_{\min} P_{\text{peak}}] \} - \mathbb{E}_{g_{\min}} \{ \log_2[1 + a_n g_{\min} P_{\text{peak}}] \}.
\end{aligned}$$

It can be noted that the preceding equation is the same as (12), with P_t^* replaced by P_{peak} . Therefore, a closed-form expression for the preceding equation can be given by (13), with P_t^* replaced by P_{peak} .

B. Outage probability

Following the arguments in Section III-B, the outage probability for the case of NOMA is defined as

$$\mathbb{P}_{\text{out}} = 1 - \Pr \left(g_n \geq \frac{\xi_n}{P_t^*(g_p)} \right) \Pr \left(g_f \geq \frac{\xi_f}{P_t^*(g_p)} \right). \quad (27)$$

Theorem 7. For the case of PowIntICSI, the outage probability for NOMA is given by (28), shown on the next page.

Proof. See Appendix G. ■

On the other hand, for the case of OMA, the outage probability is given by

$$\mathcal{P}_{\text{out}} = 1 - \prod_{u \in \{n, f\}} \Pr \left(g_u \geq \frac{\Theta}{P_t^*(g_p)} \right). \quad (29)$$

Asymptotic analysis: For the limiting case when $I \rightarrow \infty$ and P_{peak} is finite, $P_t^*(g_p)$ in (22) becomes equal to P_{peak} . Using (27), (61) and (62), it is straightforward to conclude that

$$\mathbb{P}_{\text{out}} = 1 - \prod_{u \in \{n, f\}} \frac{\Gamma[N_u, \xi_u / (\Omega_u P_{\text{peak}})]}{\Gamma(N_u)}, \quad (30)$$

which is independent of the peak tolerable interference power I . Therefore, the slope of the outage probability curve tends to zero for large values of I , resulting in a outage floor. The asymptotic expression shown above also helps to quantify the reduction in the outage floor resulting from an increase in the number of antennas at the SRs.

$$T(x) = - \left[1 - \exp \left(\frac{-I}{\Omega_p P_{\text{peak}}} \right) \right] \exp \left(\frac{1}{x P_{\text{peak}}} \right) \text{Ei} \left(\frac{-1}{x P_{\text{peak}}} \right) + \left[\text{Ei} \left(\frac{-I}{\Omega_p P_{\text{peak}}} \right) - \frac{\Omega_p}{\Omega_p - xI} \left\{ \text{Ei} \left(\frac{-I}{\Omega_p P_{\text{peak}}} \right) \right. \right. \\ \left. \left. - \exp \left(\frac{\Omega_p - xI}{x \Omega_p P_{\text{peak}}} \right) \text{Ei} \left(\frac{-1}{x P_{\text{peak}}} \right) \right\} + \exp \left(\frac{\Omega_p - xI}{x \Omega_p P_{\text{peak}}} \right) \left\{ \text{Shi} \left(\frac{1}{x P_{\text{peak}}} \right) - \text{Chi} \left(\frac{1}{x P_{\text{peak}}} \right) \right\} \right]. \quad (25)$$

$$\mathbb{P}_{\text{out}} = 1 - \left\{ \left[1 - \exp \left(\frac{-I}{\Omega_p P_{\text{peak}}} \right) \right] \prod_{u \in \{n, f\}} \frac{\Gamma[N_u, \xi_u / (\Omega_u P_{\text{peak}})]}{\Gamma(N_u)} \right. \\ \left. + \frac{1}{\Omega_p} \sum_{k=0}^{N_f-1} \sum_{l=0}^{N_n-1} \frac{\xi_n^l \xi_f^k}{k! l! \Omega_n^l \Omega_f^k I^{k+l}} \Gamma \left[k+l+1, \left(\frac{1}{\Omega_p} + \frac{\xi_n}{\Omega_n I} + \frac{\xi_f}{\Omega_f I} \right) \frac{I}{P_{\text{peak}}} \right] \left(\frac{1}{\Omega_p} + \frac{\xi_n}{\Omega_n I} + \frac{\xi_f}{\Omega_f I} \right)^{-(k+l+1)} \right\}. \quad (28)$$

C. Optimal power allocation

It can be shown that for the case of PowIntICSI, it is very complicated (if not impossible) to find a closed-form expression for a_n^* , even for the case where $N_n = N_f = 1$. Therefore, for the case of PowIntICSI, we find the optimal value of a_n numerically.

VI. SECONDARY PERFORMANCE FOR POWINTSCSI

For the analysis in this section, we assume that the power transmitted from the ST is constrained by the peak interference constraint at the PR as well as the peak power budget at the ST. Additionally, we assume that only statistical IL-CSI is available at the ST.

A. Average achievable sum-rate

The average achievable sum-rate for the case of NOMA is given by

$$C_{\text{sum}} = \max_{P_t \geq 0} \mathbb{E}_{g_n, g_f} \{ \log_2(1 + a_n P_t g_n) + \log_2(1 + P_t g_{\min}) - \log_2(1 + a_n P_t g_{\min}) \}, \quad (31)$$

$$\text{s.t. } \Pr(g_p P_t \geq I) \leq \delta, \quad (32)$$

$$P_t \leq P_{\text{peak}}. \quad (33)$$

Using (32), (33) and (11), the optimal transmit power to maximize the sum-rate for NOMA is given by

$$P_t^* = \min \left\{ P_{\text{peak}}, \frac{-I}{\Omega_p \ln \delta} \right\}. \quad (34)$$

Therefore, using (31)-(34), an expression for the average achievable sum-rate for NOMA is given by

$$C_{\text{sum}} = \mathbb{E}_{g_n} \{ \log_2(1 + a_n g_n P_t^*) \} \\ + \mathbb{E}_{g_{\min}} \{ \log_2(1 + g_{\min} P_t^*) \} - \mathbb{E}_{g_{\min}} \{ \log_2(1 + a_n g_{\min} P_t^*) \}. \quad (35)$$

Note that (35) is same as (12), however, the definition of P_t^* in (35) and (12) are different. Therefore, an analytical expression for (35) is given by (13), with P_t^* given by (34).

On the other hand, for the case of OMA, the average achievable sum-rate is given by

$$\mathcal{C}_{\text{sum}} = 0.5 \sum_{u \in \{n, f\}} \mathbb{E}_{g_u} \{ \log_2(1 + g_u P_t^*) \}, \quad (36)$$

where P_t^* is given by (34).

Asymptotic analysis: Similar to the case of PowIntICSI, a closed-form expression for the asymptotic achievable sum-rate for the PowIntSCSI NOMA system can be given by (13), with P_t^* replaced by P_{peak} . This means that for the case of NOMA, the average achievable sum-rate for both PowIntICSI and PowIntSCSI systems are exactly the same for a sufficiently large value of I and a finite value of P_{peak} . This is intuitive because when the value of I is sufficiently large, the (average) transmitted power from the ST for both systems is the same (equal to P_{peak}) and no gain is obtained from the instantaneous knowledge of the ST-PR link CSI.

B. Outage probability

Following arguments similar to those in the previous subsection, the outage probability for NOMA is given by (16), where P_t^* is given by (34).

On the other hand, for the case of OMA, the outage probability is given by

$$\mathcal{P}_{\text{out}} = 1 - \prod_{u \in \{n, f\}} \Pr \left(g_u \geq \frac{\Theta}{P_t^*} \right). \quad (37)$$

Asymptotic analysis: Following (16) and (34), an asymptotic expression for the outage probability for the case when $I \rightarrow \infty$ is given by

$$\mathbb{P}_{\text{out}} = 1 - \prod_{u \in \{n, f\}} \frac{\Gamma[N_u, \xi_u / (\Omega_u P_{\text{peak}})]}{\Gamma(N_u)}, \quad (38)$$

which is the same as for the case of PowIntICSI. This means that for the case of NOMA, the outage probability for the PowIntICSI and PowIntSCSI systems are exactly the same for a sufficiently large value of I and a finite value of P_{peak} .

C. Optimal power allocation

Since the expression for the outage probability for the NOMA system in the case of PowIntSCSI is the same as that for the case of IntSCSI with the expression for P_t^* given by (22) which is independent of a_n , therefore, following the arguments in Section IV-C, for the case where $N_n = N_f = 1$, a_n^* is given by

$$a_n^* = \frac{\Omega_f}{(1+\theta)\Omega_f - \Omega_n} - \frac{\sqrt{\Omega_n\Omega_f(1+\theta)}}{(1+\theta)\{(1+\theta)\Omega_f - \Omega_n\}}. \quad (39)$$

Similar to case in Section IV-C, a_n^* does not depend on P_{peak} , I or Ω_p .

VII. SECONDARY PERFORMANCE WITH ONE-BIT FEEDBACK

In this section, we consider the scenario where the ST does not have any CSI regarding the ST-PR link. We rather assume that the PR has instantaneous CSI regarding the ST-PR link. Also, we assume that the power transmitted from the ST is constrained by a peak interference constraint at the PR, as well as a peak power budget constraint at the ST.

Based on the peak power budget at the ST, and the peak interference constraint at the PR, the PR calculates a threshold value τ for the channel gain g_p . If the instantaneous channel gain of the ST-PR link is less than τ , the PR sends a “1” to the ST via a low-bandwidth zero-delay feedback link, and sends a “0” otherwise. For the case when ST receives a “1” from the PR, it transmits its signal to U_n and U_f with full power P_{peak} , otherwise it remains silent. Therefore, the transmit power from the ST is modeled as

$$P_t^* = \begin{cases} P_{\text{peak}}, & \text{if } g_p \leq \tau = \frac{I}{P_{\text{peak}}} \\ 0, & \text{otherwise.} \end{cases} \quad (40)$$

Note that the power transmission scheme in (40) ensures that the interference caused by the ST at the PR is either less than or equal to the peak tolerable interference at the PR or zero.

A. Average achievable sum-rate

The average achievable sum-rate for the case of NOMA is given by

$$\begin{aligned} C_{\text{sum}} &= \mathbb{E}_{g_n, g_f} \{ \log_2(1 + a_n P_t^* g_n) + \log_2(1 + P_t^* g_{\min}) \\ &\quad - \log_2(1 + a_n P_t^* g_{\min}) \} \\ &= \Pr(g_p \leq \tau) [\mathbb{E}_{g_n} \{ \log_2(1 + a_n g_n P_{\text{peak}}) \} \\ &\quad + \mathbb{E}_{g_{\min}} \{ \log_2(1 + g_{\min} P_{\text{peak}}) \} \\ &\quad - \mathbb{E}_{g_{\min}} \{ \log_2(1 + a_n g_{\min} P_{\text{peak}}) \}]. \end{aligned} \quad (41)$$

Following the steps in Appendix D, an analytical expression for (41) is given by (42), shown on the next page.

On the other hand, for the case of OMA, the average achievable sum-rate is given by

$$\mathcal{C}_{\text{sum}} = 0.5 \sum_{u \in \{n, f\}} \mathbb{E}_{g_u} \{ \log_2(1 + g_u P_t^*) \}, \quad (43)$$

where P_t^* is given by (40).

Asymptotic analysis: For the case when $I \rightarrow \infty$, the transmit power P_t^* in (40) becomes equal to P_{peak} , and $\Pr(g_p \leq \tau) \rightarrow 1$. Therefore, using (41), a closed-form expression for the asymptotic average achievable sum-rate is given by (13), with P_t^* in (13) replaced by P_{peak} .

This means that for the case when the ST has a fixed power budget, the achievable sum-rate will always converge to the same value for NOMA systems in the high- I regime, regardless of the level of IL-CSI knowledge at the ST.

B. Outage probability

Similar to Section III-B, the outage probability for the case of NOMA is given by

$$\begin{aligned} \mathbb{P}_{\text{out}} &= 1 - \Pr \left(\frac{a_f P_t^* g_n}{a_n P_t^* g_n + 1} \geq \theta, a_n P_t^* g_n \geq \theta \right) \\ &\quad \times \Pr \left(\frac{a_f P_t^* g_f}{a_n P_t^* g_f + 1} \geq \theta \right) \\ &= 1 - \Pr(g_p \leq \tau) \Pr \left(g_n \geq \frac{\xi_n}{P_{\text{peak}}} \right) \Pr \left(g_f \geq \frac{\xi_f}{P_{\text{peak}}} \right) \\ &= 1 - \left\{ 1 - \exp \left(\frac{-\tau}{\Omega_p} \right) \right\} \prod_{u \in \{n, f\}} \frac{\Gamma[N_u, \xi_u / (\Omega_u P_{\text{peak}})]}{\Gamma(N_u)}. \end{aligned} \quad (44)$$

On the other hand, for the case of OMA, the outage probability is given by

$$\mathcal{P}_{\text{out}} = 1 - \prod_{u \in \{n, f\}} \Pr \left(g_u \geq \frac{\Theta}{P_t^*} \right), \quad (45)$$

where P_t^* is given in (40).

Asymptotic analysis: For the limiting case $I \rightarrow \infty$, we have $(1 - \exp(-\tau/\Omega_p)) \rightarrow 1$. Therefore, using (44), we have

$$\mathbb{P}_{\text{out}} = 1 - \prod_{u \in \{n, f\}} \frac{\Gamma[N_u, \xi_u / (\Omega_u P_{\text{peak}})]}{\Gamma(N_u)}, \quad (46)$$

which is the same as obtained for the case of PowIntICSI and PowIntSCSI. This occurs because for the limiting case of $I \rightarrow \infty$, the ST always receives a feedback ‘1’ from the PT, and therefore, always transmits at a constant power P_{peak} .

This means that for the case when the ST has a fixed power budget, the outage floor will always be the same for NOMA systems, regardless of the level of IL-CSI knowledge at the ST.

C. Optimal power allocation

Note that the expression for the outage probability for the NOMA system in the case of PowIntOneBit given in (44) is similar to that for the case of IntSCSI given in (16), where the difference is that P_t^* in (16) is replaced by P_{peak} in (44), and there exists an extra factor of $(1 - \exp(-\tau/\Omega_p))$. Since both P_{peak} and $(1 - \exp(-\tau/\Omega_p))$ are independent of a_n , therefore, following the arguments in Section IV-C, for the case where $N_n = N_f = 1$, a_n^* is given by

$$a_n^* = \frac{\Omega_f}{(1+\theta)\Omega_f - \Omega_n} - \frac{\sqrt{\Omega_n\Omega_f(1+\theta)}}{(1+\theta)\{(1+\theta)\Omega_f - \Omega_n\}}. \quad (47)$$

Similar to case in Section IV-C, a_n^* does not depend on P_{peak} , I , Ω_p or τ .

$$\begin{aligned}
C_{\text{sum}} = & \frac{1 - \exp(-\tau/\Omega_p)}{\ln 2} \left[\frac{1}{\Gamma(N_n)\Omega_n^{N_n}(a_n P_{\text{peak}})^{N_n}} G_{2,3}^{3,1} \left(\frac{1}{\Omega_n a_n P_{\text{peak}}} \middle| \begin{matrix} -N_n, 1-N_n \\ 0, -N_n, -N_n \end{matrix} \right) + \frac{1}{\Gamma(N_n)\Omega_n^{N_n}} \sum_{k=0}^{N_f-1} \frac{1}{k! \Omega_f^k} \right. \\
& \times \frac{1}{(P_{\text{peak}})^{N_n+k}} \left\{ G_{2,3}^{3,1} \left(\frac{1}{\Omega P_{\text{peak}}} \middle| \begin{matrix} -N_n-k, 1-N_n-k \\ 0, -N_n-k, -N_n-k \end{matrix} \right) - \frac{1}{a_n^{N_n+k}} G_{2,3}^{3,1} \left(\frac{1}{\Omega a_n P_{\text{peak}}} \middle| \begin{matrix} -N_n-k, 1-N_n-k \\ 0, -N_n-k, -N_n-k \end{matrix} \right) \right\} + \frac{1}{\Gamma(N_f)\Omega_f^{N_f}} \\
& \times \sum_{l=0}^{N_n-1} \frac{1}{l! \Omega_n^l (P_{\text{peak}})^{N_f+l}} \left\{ G_{2,3}^{3,1} \left(\frac{1}{\Omega P_{\text{peak}}} \middle| \begin{matrix} -N_f-l, 1-N_f-l \\ 0, -N_f-l, -N_f-l \end{matrix} \right) - \frac{1}{a_n^{N_f+l}} G_{2,3}^{3,1} \left(\frac{1}{\Omega a_n P_{\text{peak}}} \middle| \begin{matrix} -N_f-l, 1-N_f-l \\ 0, -N_f-l, -N_f-l \end{matrix} \right) \right\} \Big]. \quad (42)
\end{aligned}$$

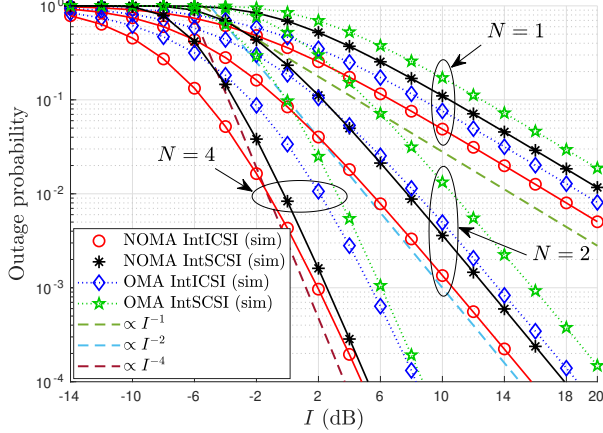


Fig. 2. Outage probability for the IntICSI and IntSCSI systems. Here solid lines are plotted using (7) and (16). The constant-slope dotted lines show the slope of \mathbb{P}_{out} for large I .

VIII. RESULTS AND DISCUSSION

In this section, we present the simulation and analytical results for the performance of the spectrum sharing NOMA/OMA systems. Throughout this section, we assume $d_n = 30\text{m}$, $d_f = 100\text{m}$, $d_p = 200\text{m}$, $\alpha = 2$, $\delta = 0.1$ and $N_n = N_f = N$. However, note that the analytical results presented in this paper are also valid for the case when $N_n \neq N_f$.

Fig. 2 shows a comparison between IntICSI and IntSCSI NOMA/OMA systems in terms of outage probability, for different values of N . It is clear from the figure that the spectrum sharing NOMA system significantly outperforms the corresponding OMA system for both IntICSI and IntSCSI cases. It is important to note that for large values of I , the difference between the outage probability of the NOMA system and the corresponding OMA system increases with an increase in the value of N . It is also noteworthy that for large values of I , the difference between the outage probability of the NOMA system for IntICSI and IntSCSI decreases with an increase in the value of N , indicating that the impact of information loss becomes less significant for larger values of N and I .

Fig. 3 shows the outage probability of the PowIntICSI system for both NOMA and OMA, with different values of N and P_{peak} . For both NOMA and OMA systems, the outage probability first decreases for small values of I (which we refer to as the *interference-constrained regime*) and then

becomes saturated for large values of I (which we refer to as the *power-constrained regime*), as is evident from (30). This occurs because the average power transmitted from the ST first increases with an increase in the value of I and when the value of I is large, the average power transmitted from the ST becomes constant, resulting in an outage floor. It is evident from the figure that the outage probability of NOMA system is significantly lower than that of the corresponding OMA system. More interestingly, for the NOMA/OMA system, the outage probability remains (almost) the same in the interference-constrained regime for a fixed value of N , regardless of the value of P_{peak} , whereas the effect of P_{peak} becomes significantly evident in the power-constrained regime.

The outage probability of the PowIntSCSI NOMA/OMA system is shown in Fig. 4 for different values of N and P_{peak} . Similar to the case of Fig. 3, the interference-constrained regime and power-constrained regime (see (38)) are clearly evident in Fig. 4, with the NOMA system outperforming the corresponding OMA system. However, different from the case in Fig. 3, the outage probability of NOMA/OMA for a fixed value of N is *exactly* the same in the interference-constrained regime, irrespective of the value of P_{peak} . This occurs because the power transmitted by the ST is given by $P_t^* = \min\{P_{\text{peak}}, -I/(\Omega_p \ln \delta)\}$; in the interference-constrained regime, this is equal to $-I/(\Omega_p \ln \delta)$, which is independent of P_{peak} .

Fig. 5 depicts the outage probability performance of the PowIntOneBit NOMA/OMA systems for different values of N and P_{peak} . It is clearly evident from the figure that the NOMA system outperforms its OMA-based counterpart, by achieving a lower outage probability. However, different from the case in Figs. 3 and 4, for a fixed value of N , the outage probability of NOMA/OMA systems with larger value of P_{peak} is higher in the interference-constrained regime. This occurs because when the value of P_{peak} is large (for a fixed N), the value of $\tau \triangleq I/P_{\text{peak}}$ becomes small and therefore, the probability of receiving a feedback “1” at the ST becomes smaller (c.f. (40)), which in turn leads to a higher probability of the ST being silent. Therefore, different from the other cases, having a higher peak power budget is not always beneficial in the interference-constrained regime for the case of the PowIntOneBit system. However, in the power-constrained regime (see (46)), having a large P_{peak} is always advantageous, as is evident from the figure.

Fig. 6 shows a comparison of the outage probability for PowIntICSI, PowIntSCSI and PowIntOneBit NOMA systems

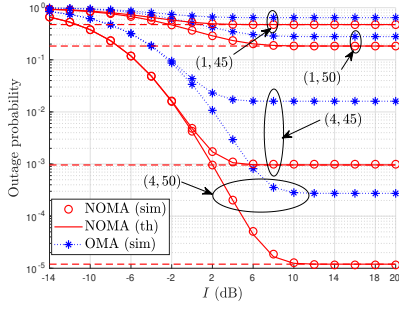


Fig. 3. Outage probability for the PowIntICSI system. The solid lines are drawn using (28). The tuples in the parenthesis denote (N, P_{peak}) , and the horizontal dotted lines drawn using (30) denote the asymptotic \mathbb{P}_{out} for the NOMA system.

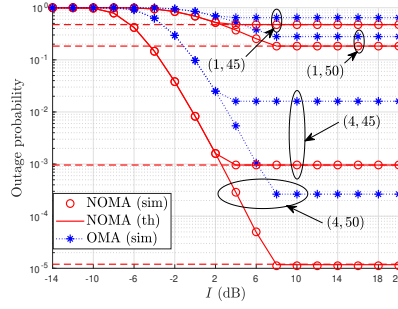


Fig. 4. Outage probability for the PowIntSCSI system. The solid lines are drawn using (16) with P_t^* given by (34). The tuples in the parenthesis denote (N, P_{peak}) , and the horizontal dotted lines drawn using (38) denote the asymptotic \mathbb{P}_{out} for the NOMA system.

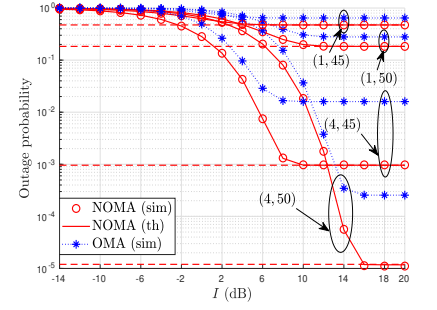


Fig. 5. Outage probability for the PowIntOneBit system. The solid lines are drawn using (44). The tuples in the parenthesis denote (N, P_{peak}) , and the horizontal dotted lines drawn using (46) denote the asymptotic \mathbb{P}_{out} for the NOMA system.

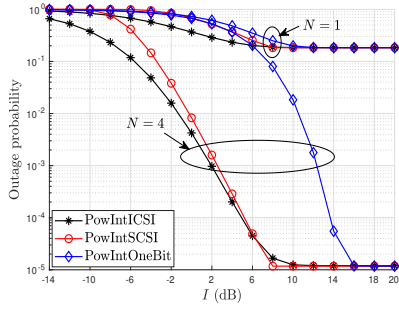


Fig. 6. Analytical plots for the outage probability of the PowIntICSI, PowIntSCSI and PowIntOneBit NOMA systems. Here P_{peak} is fixed at 50 dB.

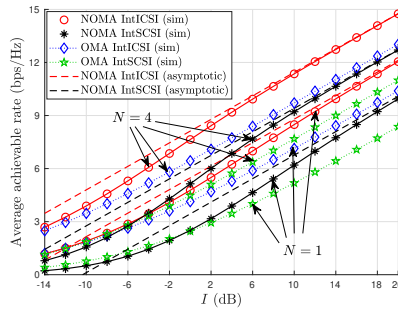


Fig. 7. Average achievable sum-rate for the IntICSI and IntSCSI systems. Here solid lines are plotted using (4) and (13), while the dotted lines are drawn using (6) and (15).

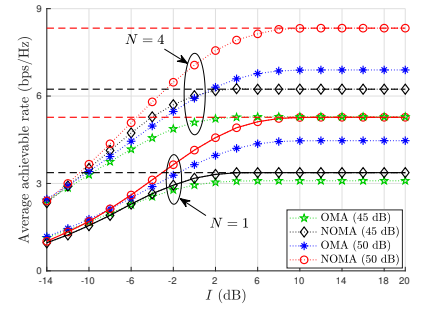


Fig. 8. Average achievable sum-rate for the PowIntICSI system. Here markers with dotted lines represent the simulation results, the solid lines drawn using (24) represent the analytical results, and the horizontal dotted lines drawn using (13) with P_t^* replaced by P_{peak} , denote the asymptotic results (for NOMA).

with $P_{\text{peak}} = 50$ dB. It is evident from the figure that in the power-constrained regime, the outage probability for all the three NOMA systems for a fixed value of N converges to the same outage floor, in accordance with the asymptotic analysis of the outage probability of the corresponding systems. In the interference-constrained regime, the effect of information loss in terms of IL-CSI between PowIntICSI and PowIntSCSI systems is not very significant. However, in the case of PowIntOneBit system, the effect of information loss in terms of IL-CSI becomes significantly dominant in the interference-constrained regime, especially for large N .

Fig. 7 shows a comparison of the average achievable sum-rate for IntICSI and IntSCSI NOMA and OMA systems. It is evident from the figure that the NOMA-based system outperforms the corresponding OMA-based system in terms of achievable sum-rate for large values of N . It is noteworthy that in contrast to the behavior in the case of outage probability, the performance degradation in IntSCSI system as compared to IntICSI system in terms of achievable rate due to information loss is significant even for large values of N . We have also plotted the asymptotic sum-rate for the NOMA system using (6) for IntICSI and (15) for IntSCSI, which shows a close agreement with the exact sum-rate for large I .

In Fig. 8, the average achievable sum-rate for the PowIn-

IntICSI NOMA/OMA system is shown for different values of N and P_{peak} . Interestingly, the difference between the sum-rate of the NOMA systems with $P_{\text{peak}} = 45$ dB and 50 dB is less significant in the interference-constrained regime, whereas the performance difference between the two systems becomes significant in the power-constrained regime.

Fig. 9 shows the average achievable sum-rate for PowIntSCSI NOMA and OMA systems for different values of N and P_{peak} . It is noteworthy from the figure that for a fixed N in the interference-constrained regime, the sum-rate for the NOMA/OMA system is *exactly* the same for both $P_{\text{peak}} = 45$ dB and 50 dB, because of the same reason as explained previously for Fig. 4. Also, as explained for the previous figure, the achievable rate for both NOMA and OMA systems saturates in the power-constrained regime (see (13), with P_t^* replaced by P_{peak}) for NOMA, due to the fact that the power transmitted from the ST is constant and independent of the value of I .

Fig. 10 depicts the average achievable sum-rate performance of the PowIntOneBit NOMA and OMA systems for different values of N and P_{peak} . For a fixed value of N in the interference-constrained regime, the sum-rate of the NOMA/OMA system with larger P_{peak} achieves lower sum-rate as compared to the NOMA/OMA system with smaller

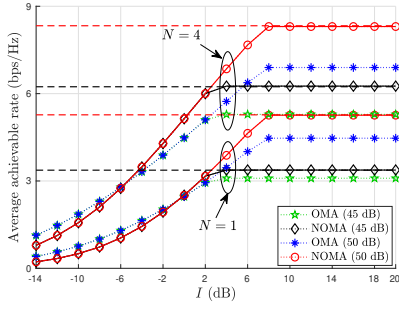


Fig. 9. Average achievable sum-rate for the PowIntSCSI system. Markers with dotted lines represent the simulation results, the solid lines drawn using (13) with P_t^* given by (34) represent the analytical results, and the horizontal dotted lines drawn using (13), with P_t^* replaced by P_{peak} , denote the asymptotic results (for NOMA).

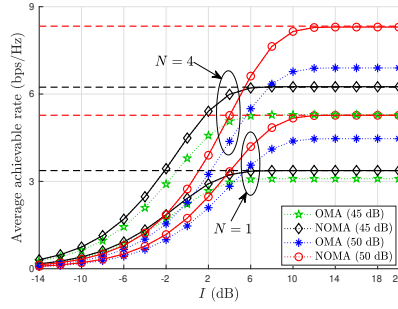


Fig. 10. Average achievable sum-rate for the PowIntOneBit system. Markers with dotted lines represent the simulation results, the solid lines drawn using (42) denote the analytical results, and the horizontal dotted lines drawn using (13), with P_t^* replaced by P_{peak} , represent asymptotic results (for NOMA).

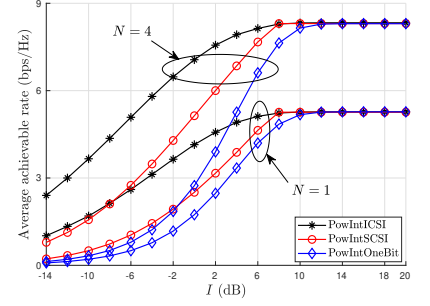


Fig. 11. Analytical plots for the average achievable sum-rate of the PowIntICSI, PowIntSCSI and PowIntOneBit NOMA systems. Here P_{peak} is fixed at 50 dB.

P_{peak} , because of the same reason as explained previously for Fig. 5. Therefore, having a higher peak power budget in the PowIntOneBit NOMA/OMA system is not always beneficial in the interference-constrained regime. However, in the power-constrained regime, a larger value of P_{peak} results in a higher achievable sum-rate.

Fig. 11 shows the achievable sum-rate performance of PowIntICSI, PowIntSCSI and PowIntOneBit NOMA systems for the case when $P_{\text{peak}} = 50$ dB. It can be noticed from the figure that in the interference-constrained regime, there is a significant performance degradation due to the information loss in terms of IL-CSI, whereas in the power-constrained regime, there is no effect of information loss in terms of IL-CSI.

IX. CONCLUSION

In this paper, we presented the performance analysis of a multi-antenna-assisted NOMA-based underlay spectrum sharing system over Rayleigh fading channels. We derived closed-form expressions for the average achievable sum-rate and outage probability for the downlink NOMA system under a peak interference as well as a peak power budget constraint with different CSI availability at the ST regarding the link between ST and PR. Our results confirm that for a large number of antennas at the secondary users, the performance difference between the system with instantaneous IL-CSI and statistical IL-CSI in the interference-constrained regime is negligible in terms of outage probability, whereas this difference is significant in terms of achievable sum-rate. On the other hand when no IL-CSI is available at the ST, the NOMA and OMA systems both suffer from a significant performance degradation in the interference-constrained regime for a large number of antennas, in terms of outage probability as well as achievable sum-rate. However, in the power-constrained regime, the effect of information loss in IL-CSI is negligible for both outage probability and achievable sum-rate. We also derived closed-form expressions for the optimal power allocation to minimize the outage probability of NOMA systems for the special case when the secondary users are each equipped with a single antenna.

APPENDIX A PROOF OF THEOREM 1

Given that channel gains for all of the wireless links are exponential distributed, the PDF and CDF of $g_u (u \in \{n, f\})$, are respectively given by

$$f_{g_u}(x) = \frac{x^{N_u-1}}{\Gamma(N_u)\Omega_u^{N_u}} \exp\left(-\frac{x}{\Omega_u}\right), \quad (48)$$

and

$$F_{g_u}(x) = 1 - \exp\left(-\frac{x}{\Omega_u}\right) \sum_{k=0}^{N_u-1} \frac{1}{k!} \left(\frac{x}{\Omega_u}\right)^k. \quad (49)$$

Also, the PDF of g_p is given by

$$f_{g_p}(x) = \frac{1}{\Omega_p} \exp\left(-\frac{x}{\Omega_p}\right). \quad (50)$$

Now, the PDF of g_{\min} can be obtained by

$$\begin{aligned} f_{g_{\min}}(x) &= f_{g_n}(x)[1 - F_{g_f}(x)] + f_{g_f}(x)[1 - F_{g_n}(x)] \\ &= \frac{1}{\Gamma(N_n)\Omega_n^{N_n}} \sum_{k=0}^{N_f-1} \frac{x^{N_n+k-1}}{k!\Omega_f^k} \exp\left(-\frac{x}{\Omega_f}\right) \\ &\quad + \frac{1}{\Gamma(N_f)\Omega_f^{N_f}} \sum_{l=0}^{N_n-1} \frac{x^{N_f+l-1}}{l!\Omega_n^l} \exp\left(-\frac{x}{\Omega_n}\right). \end{aligned} \quad (51)$$

Also, the PDF of $X_u \triangleq g_u/g_p$ can be obtained as

$$\begin{aligned} f_{X_u}(x) &= \int_0^\infty y f_{g_u}(yx) f_{g_p}(y) dy \\ &= \frac{x^{N_u-1}}{\Gamma(N_u)\Omega_u^{N_u}\Omega_p} \int_0^\infty y^{N_u} \exp\left[-\left(\frac{x}{\Omega_u} + \frac{1}{\Omega_p}\right)y\right] dy \\ &= \frac{N_u x^{N_u-1}}{\Omega_u^{N_u}\Omega_p} \left(\frac{x}{\Omega_u} + \frac{1}{\Omega_p}\right)^{-(N_u+1)}, \end{aligned} \quad (52)$$

where the integration above is solved using [22, eqn. (3.351-3), p. 340]. Similarly, the PDF of $X_{\min} \triangleq g_{\min}/g_p$ can be given by

$$f_{X_{\min}}(x) = \int_0^\infty y f_{g_{\min}}(yx) f_{g_p}(y) dy$$

$$\begin{aligned}
&= \frac{1}{\Gamma(N_n)\Omega_n^{N_n}\Omega_p} \sum_{k=0}^{N_f-1} \frac{x^{N_n+k-1}}{k!\Omega_f^k} \int_0^\infty y^{N_n+k} \\
&\quad \times \exp\left[-\left(\frac{x}{\Omega} + \frac{1}{\Omega_p}\right)y\right] dy + \frac{1}{\Gamma(N_f)\Omega_f^{N_f}\Omega_p} \\
&\quad \times \sum_{l=0}^{N_n-1} \frac{x^{N_f+l-1}}{l!\Omega_n^l} \int_0^\infty y^{N_f+l} \exp\left[-\left(\frac{x}{\Omega} + \frac{1}{\Omega_p}\right)y\right] dy \\
&= \sum_{k=0}^{N_f-1} \frac{x^{N_n+k-1}\Gamma(N_n+k+1)}{\Gamma(N_n)k!\Omega_n^{N_n}\Omega_f^k\Omega_p} \left(\frac{x}{\Omega} + \frac{1}{\Omega_p}\right)^{-(N_n+k+1)} \\
&\quad + \sum_{l=0}^{N_n-1} \frac{x^{N_f+l-1}\Gamma(N_f+l+1)}{\Gamma(N_f)l!\Omega_f^{N_f}\Omega_n^l\Omega_p} \left(\frac{x}{\Omega} + \frac{1}{\Omega_p}\right)^{-(N_f+l+1)}. \tag{53}
\end{aligned}$$

The integration above is solved using [22, eqn. (3.351-3), p. 340]. Using (52), an analytical expression for the first expectation in (3) is be given by

$$\begin{aligned}
\mathbb{E}_{X_n}\{\log_2(1+a_nIX_n)\} &= \frac{1}{\ln 2} \int_0^\infty \ln(1+a_nIx) f_{X_n}(x) dx \\
&= \frac{N_n\Omega_p^{N_n}}{\Omega_n^{N_n} \ln 2} \int_0^\infty x^{N_n-1} \ln(1+a_nIx) \left(1 + \frac{\Omega_p}{\Omega_n}x\right)^{-(N_n+1)} dx \\
&= \frac{N_n\Omega_p^{N_n}}{\Omega_n^{N_n}\Gamma(N_n+1) \ln 2} \int_0^\infty x^{N_n-1} G_{2,2}^{1,2}\left(a_nIx \middle| \begin{smallmatrix} 1, 1 \\ 1, 0 \end{smallmatrix}\right) \\
&\quad \times G_{1,1}^{1,1}\left(\frac{\Omega_p}{\Omega_n}x \middle| \begin{smallmatrix} -N_n \\ 0 \end{smallmatrix}\right) dx \\
&= \frac{1}{\Gamma(N_n) \ln 2} \left(\frac{\Omega_p}{\Omega_n a_n I}\right)^{N_n} G_{3,3}^{3,2}\left(\frac{\Omega_p}{\Omega_n a_n I} \middle| \begin{smallmatrix} -N_n, -N_n, 1-N_n \\ 0, -N_n, -N_n \end{smallmatrix}\right), \tag{54}
\end{aligned}$$

where the integration above is solved using [24, eqns. (7), (11), (21), and (22)]. Similarly, using (53), an analytical expression for the second expectation in (3) is given by

$$\begin{aligned}
\mathbb{E}_{X_{\min}}\{\log_2(1+IX_{\min})\} &= \frac{1}{\ln 2} \left[\sum_{k=0}^{N_f-1} \frac{\Gamma(N_n+k+1)}{\Gamma(N_n)k!\Omega_n^{N_n}\Omega_f^k\Omega_p} \int_0^\infty x^{N_n+k-1} \ln(1+Ix) \right. \\
&\quad \times \left(\frac{x}{\Omega} + \frac{1}{\Omega_p}\right)^{-(N_n+k+1)} dx + \sum_{l=0}^{N_n-1} \frac{\Gamma(N_f+l+1)}{\Gamma(N_f)l!\Omega_f^{N_f}\Omega_n^l\Omega_p} \\
&\quad \times \int_0^\infty x^{N_f+l-1} \ln(1+Ix) \left(\frac{x}{\Omega} + \frac{1}{\Omega_p}\right)^{-(N_f+l+1)} dx \Big] \\
&= \frac{1}{\ln 2} \left[\sum_{k=0}^{N_f-1} \frac{\Omega_p^{N_n+k}}{\Gamma(N_n)k!\Omega_n^{N_n}\Omega_f^k} \int_0^\infty x^{N_n+k-1} G_{2,2}^{1,2}\left(Ix \middle| \begin{smallmatrix} 1, 1 \\ 1, 0 \end{smallmatrix}\right) \right. \\
&\quad \times G_{1,1}^{1,1}\left(\frac{\Omega_p}{\Omega}x \middle| \begin{smallmatrix} -N_n-k \\ 0 \end{smallmatrix}\right) dx + \sum_{l=0}^{N_n-1} \frac{\Omega_p^{N_f+l}}{\Gamma(N_f)l!\Omega_f^{N_f}\Omega_n^l} \\
&\quad \times \int_0^\infty x^{N_f+l-1} G_{2,2}^{1,2}\left(Ix \middle| \begin{smallmatrix} 1, 1 \\ 1, 0 \end{smallmatrix}\right) G_{1,1}^{1,1}\left(\frac{\Omega_p}{\Omega}x \middle| \begin{smallmatrix} -N_f-l \\ 0 \end{smallmatrix}\right) dx \Big]
\end{aligned}$$

$$\begin{aligned}
&= \frac{1}{\ln 2} \left[\sum_{k=0}^{N_f-1} \frac{\Omega_p^{N_n+k} G_{3,3}^{3,2}\left(\frac{\Omega_p}{\Omega I} \middle| \begin{smallmatrix} -N_n-k, -N_n-k, 1-N_n-k \\ 0, -N_n-k, -N_n-k \end{smallmatrix}\right)}{\Gamma(N_n)k!\Omega_n^{N_n}\Omega_f^k I^{N_n+k}} \right. \\
&\quad \left. + \sum_{l=0}^{N_n-1} \frac{\Omega_p^{N_f+l} G_{3,3}^{3,2}\left(\frac{\Omega_p}{\Omega I} \middle| \begin{smallmatrix} -N_f-l, -N_f-l, 1-N_f-l \\ 0, -N_f-l, -N_f-l \end{smallmatrix}\right)}{\Gamma(N_f)l!\Omega_f^{N_f}\Omega_n^l I^{N_f+l}} \right]. \tag{55}
\end{aligned}$$

The integral above is solved in a similar fashion as in (54). An analytical expression for the third expectation in (3) can be obtained by replacing I with $a_n I$ in (55). Therefore, using (54) and (55), an analytical expression for (3) is given by (4); this concludes the proof.

APPENDIX B PROOF OF THEOREM 2

We first define the *non-outage* event for NOMA as the event where x_f and x_n are decoded successfully at U_n , and x_f is decoded successfully at U_f . Therefore, the outage probability for the NOMA system is given by

$$\begin{aligned}
\mathbb{P}_{\text{out}} &= 1 - \Pr\left(\gamma_n^{(f)} \geq \theta, \gamma_n^{(n)} \geq \theta\right) \Pr\left(\gamma_f^{(f)} \geq \theta\right) \\
&= 1 - \Pr\left(\frac{a_f I g_n / g_p}{1 + a_n I g_n / g_p} \geq \theta, \frac{a_n I g_n}{g_p} \geq \theta\right) \\
&\quad \times \Pr\left(\frac{a_f I g_f / g_p}{1 + a_n I g_f / g_p} \geq \theta\right) \\
&= 1 - \Pr\left(\frac{a_f I X_n}{1 + a_n I X_n} \geq \theta, a_n I X_n \geq \theta\right) \\
&\quad \times \Pr\left(\frac{a_f I X_f}{1 + a_n I X_f} \geq \theta\right) \\
&= 1 - \Pr\left(X_n \geq \frac{\theta}{I} \max\left\{\frac{1}{a_f - a_n \theta}, \frac{1}{a_n}\right\}\right) \\
&\quad \times \Pr\left(X_f \geq \frac{\theta}{I(a_f - a_n \theta)}\right).
\end{aligned}$$

Using the relations $\xi_n = \theta \max\left\{\frac{1}{a_f - a_n \theta}, \frac{1}{a_n}\right\}$ and $\xi_f = \frac{\theta}{a_f - a_n \theta}$, the expression for \mathbb{P}_{out} can be written as

$$\begin{aligned}
\mathbb{P}_{\text{out}} &= 1 - \Pr\left(X_n \geq \frac{\xi_n}{I}\right) \Pr\left(X_f \geq \frac{\xi_f}{I}\right) \\
&= 1 - \prod_{u \in \{n, f\}} \mathcal{F}_{X_u}\left(\frac{\xi_u}{I}\right), \tag{56}
\end{aligned}$$

where $\mathcal{F}_{X_u}(\cdot)$ is evaluated as

$$\begin{aligned}
\mathcal{F}_{X_u}\left(\frac{\xi_u}{I}\right) &= \int_{\xi_u/I}^\infty f_{X_u}(x) dx \\
&= \frac{N_u \Omega_u}{\Omega_p} \int_{\xi_u/I}^\infty x^{N_u-1} \left(x + \frac{\Omega_u}{\Omega_p}\right)^{-(N_u+1)} dx \\
&= 1 - \left(\frac{\Omega_p \xi_u}{\Omega_u I + \Omega_p \xi_u}\right)^{N_u}. \tag{57}
\end{aligned}$$

Substituting the expression for $\mathcal{F}_{X_u}(\xi_u/I)$ from (57) into (56), the closed-form expression for \mathbb{P}_{out} becomes equal to (7); this concludes the proof.

APPENDIX C
PROOF OF THEOREM 3

For the case where $N_n = N_f = 1$, the outage probability is given by

$$\mathbb{P}_{\text{out}} = 1 - \prod_{u \in \{n, f\}} \frac{\Omega_u}{\Omega_u + \Omega_p(\xi_u/I)}.$$

Assuming, $1/(a_f - a_n\theta) > 1/a_n$, i.e., $\xi_n = 1/(1 - a_n - a_n\theta)$, we have

$$\begin{aligned} \frac{\partial \mathbb{P}_{\text{out}}}{\partial a_n} &= \frac{I^2 \Omega_p \Omega_n \Omega_f \theta (1 + \theta) (a_n + a_n\theta - 1)}{\{\Omega_p \theta - I \Omega_n (a_n + a_n\theta - 1)\}^2} \\ &\times \frac{\{I(\Omega_n + \Omega_f)(a_n + a_n\theta - 1) - 2\Omega_p \theta\}}{\{\Omega_p \theta - I \Omega_f (a_n + a_n\theta - 1)\}^2}. \end{aligned}$$

Using the fact that $a_n < 1/(1 + \theta)$ (see Section III-B), we have

$$\begin{aligned} \frac{\partial \mathbb{P}_{\text{out}}}{\partial a_n} &= 0 \\ \implies I(\Omega_f + \Omega_n) \{(1 + \theta)a_n - 1\}^2 \\ &- 2\theta \Omega_p \{(1 + \theta)a_n - 1\} = 0. \end{aligned}$$

The preceding equation is quadratic, leading to the following two solutions:

$$a_n = \frac{1}{1 + \theta}, \quad \frac{1}{1 + \theta} + \frac{2\Omega_p \theta}{I(\Omega_n + \Omega_f)(1 + \theta)}.$$

Since, $a_n < 1/(1 + \theta)$, neither of the above optimal values is feasible. Now assuming that $1/(a_f - a_n\theta) < 1/a_n$, i.e., $\xi_n = 1/a_n$, we have

$$\begin{aligned} \frac{\partial \mathbb{P}_{\text{out}}}{\partial a_n} &= \frac{I^2 \Omega_p \Omega_n \Omega_f \theta}{(a_n I \Omega_n + \Omega_p \theta)^2 \{\Omega_p \theta - I \Omega_f (a_n + a_n\theta - 1)\}^2} \\ &\times \{-I \Omega_f - \Omega_p \theta + 2a_n(1 + \theta)(I \Omega_f + \Omega_p \theta) \\ &- a_n^2 I(1 + \theta)(-\Omega_n + \Omega_f + \Omega_f \theta)\} \end{aligned}$$

Since $a_n < 1/(1 + \theta)$, we have

$$\begin{aligned} \frac{\partial \mathbb{P}_{\text{out}}}{\partial a_n} &= 0 \\ \implies I^2 \Omega_p \Omega_n \Omega_f \theta \{-I \Omega_f - \Omega_p \theta + 2a_n(1 + \theta)(I \Omega_f + \Omega_p \theta) \\ &- a_n^2 I(1 + \theta)(-\Omega_n + \Omega_f + \Omega_f \theta)\} = 0 \\ \implies a_n^2 I(1 + \theta)(-\Omega_n + \Omega_f + \Omega_f \theta) \\ &- 2a_n(1 + \theta)(I \Omega_f + \Omega_p \theta) + I \Omega_f + \Omega_p \theta = 0 \\ \implies a_n &= \frac{I \Omega_f + \Omega_p \theta}{I\{(1 + \theta)\Omega_f - \Omega_n\}} \\ &\pm \frac{\sqrt{(1 + \theta)(I \Omega_f + \Omega_p \theta)\{I \Omega_n + \Omega_p \theta(1 + \theta)\}}}{I(1 + \theta)\{(1 + \theta)\Omega_f - \Omega_n\}}. \end{aligned}$$

Define

$$\begin{aligned} a_n^{(1)} &\triangleq \frac{I \Omega_f + \Omega_p \theta}{I\{(1 + \theta)\Omega_f - \Omega_n\}} \\ &+ \frac{\sqrt{(1 + \theta)(I \Omega_f + \Omega_p \theta)\{I \Omega_n + \Omega_p \theta(1 + \theta)\}}}{I(1 + \theta)\{(1 + \theta)\Omega_f - \Omega_n\}} \\ &= \frac{1}{(1 + \theta) - (\Omega_n/\Omega_f)} + \frac{\Omega_p \theta / (I \Omega_f)}{(1 + \theta) - (\Omega_n/\Omega_f)} \end{aligned}$$

$$\begin{aligned} &+ \frac{\sqrt{\frac{(I \Omega_f + \Omega_p \theta)}{I^2(1 + \theta)\Omega_f^2} \{I \Omega_n + \Omega_p \theta(1 + \theta)\}}}{(1 + \theta) - (\Omega_n/\Omega_f)} \\ &\triangleq \mathcal{X}_1 + \mathcal{X}_2 + \mathcal{X}_3. \end{aligned}$$

For the case $1 + \theta > \Omega_n/\Omega_f$, $\mathcal{X}_1, \mathcal{X}_2, \mathcal{X}_3 > 0$ and $\mathcal{X}_1 > 1/(1 + \theta)$. Therefore, $a_n^{(1)} > 1/(1 + \theta)$. On the other hand, if $1 + \theta < \Omega_n/\Omega_f$, $\mathcal{X}_1, \mathcal{X}_2, \mathcal{X}_3 < 0$ and $a_n^{(1)} < 0$. Therefore, the only feasible solution for the optimal value of a_n is

$$\begin{aligned} a_n^* &= a_n^{(2)} = \frac{I \Omega_f + \Omega_p \theta}{I\{(1 + \theta)\Omega_f - \Omega_n\}} \\ &- \frac{\sqrt{(1 + \theta)(I \Omega_f + \Omega_p \theta)\{I \Omega_n + \Omega_p \theta(1 + \theta)\}}}{I(1 + \theta)\{(1 + \theta)\Omega_f - \Omega_n\}}. \end{aligned}$$

This concludes the proof.

APPENDIX D
PROOF OF THEOREM 4

Using (48), an analytical expression for the first expectation in (12) can be given by

$$\begin{aligned} &\mathbb{E}_{g_n} \{\log_2(1 + a_n g_n P_t^*)\} \\ &= \frac{1}{\Gamma(N_n) \Omega_n^{N_n} \ln 2} \int_0^\infty x^{N_n-1} \ln(1 + a_n P_t^* x) \exp\left(\frac{-x}{\Omega_n}\right) dx \\ &= \frac{1}{\Gamma(N_n) \Omega_n^{N_n} \ln 2} \int_0^\infty x^{N_n-1} G_{2,2}^{1,2}(a_n P_t^* x \mid \frac{1}{1}, \frac{1}{0}) \\ &\quad \times G_{0,1}^{1,0}\left(\frac{x}{\Omega_n} \mid \frac{-}{0}\right) dx \\ &= \frac{G_{2,3}^{3,1}\left(\frac{1}{\Omega_n a_n P_t^*} \mid \begin{matrix} -N_n, 1-N_n \\ 0, -N_n, -N_n \end{matrix}\right)}{\Gamma(N_n) \Omega_n^{N_n} (a_n P_t^*)^{N_n} \ln 2}. \end{aligned} \quad (58)$$

The integral above is solved using [24, eqns. (7), (11), (21), and (22)]. Using (51), an analytical expression for the second expectation in (12) can be given by

$$\begin{aligned} &\mathbb{E}_{g_{\min}} \{\log_2(1 + g_{\min} P_t^*)\} \\ &= \frac{1}{\Gamma(N_n) \Omega_n^{N_n} \ln 2} \sum_{k=0}^{N_f-1} \frac{1}{k! \Omega_f^k} \int_0^\infty x^{N_n+k-1} \ln(1 + P_t^* x) \\ &\quad \times \exp\left(\frac{-x}{\Omega}\right) dx + \frac{1}{\Gamma(N_f) \Omega_f^{N_f} \ln 2} \sum_{l=0}^{N_n-1} \frac{1}{l! \Omega_n^l} \\ &\quad \times \int_0^\infty x^{N_f+l-1} \ln(1 + P_t^* x) \exp\left(\frac{-x}{\Omega}\right) dx \\ &= \frac{1}{\Gamma(N_n) \Omega_n^{N_n} \ln 2} \sum_{k=0}^{N_f-1} \frac{G_{2,3}^{3,1}\left(\frac{1}{\Omega P_t^*} \mid \begin{matrix} -N_n-k, 1-N_n-k \\ 0, -N_n-k, -N_n-k \end{matrix}\right)}{k! \Omega_f^k (P_t^*)^{N_n+k}} \\ &\quad + \frac{1}{\Gamma(N_f) \Omega_f^{N_f} \ln 2} \times \sum_{l=0}^{N_n-1} \frac{G_{2,3}^{3,1}\left(\frac{1}{\Omega P_t^*} \mid \begin{matrix} -N_f-l, 1-N_f-l \\ 0, -N_f-l, -N_f-l \end{matrix}\right)}{l! \Omega_n^l (P_t^*)^{N_f+l}}. \end{aligned} \quad (59)$$

The integrals above are solved using [24, eqns. (7), (11), (21), and (22)]. An analytical expression for the third expectation in (12) can be obtained by replacing P_t^* by $a_n P_t^*$ in (59). Therefore, using (58) and (59), an analytical expression for (12) is given by (13); this completes the proof.

APPENDIX E PROOF OF THEOREM 5

Using the relation $\Gamma[1, x] = \exp(-x)$, the expression for the outage probability for the case when $N_n = N_f = 1$ is given by

$$\mathbb{P}_{\text{out}} = 1 - \exp \left\{ - \left(\frac{\xi_n}{P_t^* \Omega_n} + \frac{\xi_f}{P_t^* \Omega_f} \right) \right\}.$$

Assuming $1/(a_f - a_n\theta) > 1/a_n$, i.e., $\xi_n = 1/(1 - a_n - a_n\theta)$, we have

$$\begin{aligned} \frac{\partial \mathbb{P}_{\text{out}}}{\partial a_n} &= \exp \left\{ \frac{-\theta(\Omega_n + \Omega_f)}{P_t^*(1 - a_n - a_n\theta)\Omega_n\Omega_f} \right\} \\ &\quad \times \frac{(\Omega_n + \Omega_f)(1 + \theta)\theta}{\Omega_n\Omega_f P_t^*(-1 + a_n + a_n\theta)^2}. \end{aligned}$$

Since $a_n < 1/(1 + \theta)$, this implies that

$$\exp \left\{ \frac{-\theta(\Omega_n + \Omega_f)}{P_t^*(1 - a_n - a_n\theta)\Omega_n\Omega_f} \right\} \neq 0.$$

Therefore,

$$\begin{aligned} \frac{\partial \mathbb{P}_{\text{out}}}{\partial a_n} &= 0 \\ \implies \frac{(\Omega_n + \Omega_f)(1 + \theta)\theta}{\Omega_n\Omega_f P_t^*(-1 + a_n + a_n\theta)^2} &= 0. \end{aligned}$$

It can easily be noticed that the only feasible solution for the above equation is $a_n = \pm\infty$.

On the other hand, when $1/(a_f - a_n\theta) < 1/a_n$, i.e., $\xi_n = 1/a_n$, we have

$$\begin{aligned} \frac{\partial \mathbb{P}_{\text{out}}}{\partial a_n} &= - \exp \left\{ - \left(\frac{\theta}{\Omega_n P_t^* a_n} + \frac{\theta}{\Omega_f P_t^*(1 - a_n - a_n\theta)} \right) \right\} \\ &\quad \times \left\{ \frac{\theta}{\Omega_n P_t^* a_n^2} - \frac{(1 + \theta)\theta}{\Omega_f P_t^*(1 - a_n - a_n\theta)^2} \right\}. \end{aligned}$$

Since $a_n < 1/(1 + \theta)$, this implies that

$$\exp \left\{ - \left(\frac{\theta}{\Omega_n P_t^* a_n} + \frac{\theta}{\Omega_f P_t^*(1 - a_n - a_n\theta)} \right) \right\} \neq 0.$$

Therefore, using the constraint $0 < a_n < 1/(1 + \theta)$, we have

$$\begin{aligned} \frac{\partial \mathbb{P}_{\text{out}}}{\partial a_n} &= 0 \implies a_n^2(1 + \theta)\{(1 + \theta)\Omega_f - \Omega_n\} \\ &\quad - 2a_n\Omega_f(1 + \theta) + \Omega_f = 0 \\ \implies a_n &= \frac{\Omega_f}{(1 + \theta)\Omega_f - \Omega_n} \pm \frac{\sqrt{\Omega_n\Omega_f(1 + \theta)}}{(1 + \theta)\{(1 + \theta)\Omega_f - \Omega_n\}}. \end{aligned}$$

Define

$$\begin{aligned} a_n^{(1)} &= \frac{\Omega_f}{(1 + \theta)\Omega_f - \Omega_n} + \frac{\sqrt{\Omega_n\Omega_f(1 + \theta)}}{(1 + \theta)\{(1 + \theta)\Omega_f - \Omega_n\}} \\ &= \frac{1}{(1 + \theta) - (\Omega_n/\Omega_f)} + \frac{\sqrt{\frac{\Omega_n}{(1 + \theta)\Omega_f}}}{(1 + \theta) - (\Omega_n/\Omega_f)} \\ &\triangleq \mathcal{X}_1 + \mathcal{X}_2. \end{aligned}$$

For the case when $1 + \theta > \Omega_n/\Omega_f$, $\mathcal{X}_1, \mathcal{X}_2 > 0$ and $\mathcal{X}_1 > 1/(1 + \theta)$, leading to $a_n^{(1)} > 1/(1 + \theta)$. On the other hand, if

$1 + \theta < \Omega_n/\Omega_f$, $\mathcal{X}_1, \mathcal{X}_2 < 0$, leading to $a_n^{(1)} < 0$. Therefore, the only feasible solution is given by

$$a_n^* = a_n^{(2)} = \frac{\Omega_f}{(1 + \theta)\Omega_f - \Omega_n} - \frac{\sqrt{\Omega_n\Omega_f(1 + \theta)}}{(1 + \theta)\{(1 + \theta)\Omega_f - \Omega_n\}}.$$

This completes the proof.

APPENDIX F PROOF OF THEOREM 6

Given that $N_n = N_f = 1$, we have $g_n = |h_{n,1}|^2$ and $g_f = |h_{f,1}|^2$. The expressions for the PDFs of g_u and g_{\min} are respectively given by

$$f_{g_u}(x) = \frac{1}{\Omega_u} \exp \left(\frac{-x}{\Omega_u} \right), \quad f_{g_{\min}}(x) = \frac{1}{\Omega} \exp \left(\frac{-x}{\Omega} \right).$$

Solving the first expectation in (23), we have

$$\begin{aligned} &\mathbb{E}_{g_p, g_n} \{ \log_2[1 + a_n g_n P_t^*(g_p)] \} \\ &= \int_{y=0}^{y=\frac{I}{P_{\text{peak}}}} \int_{x=0}^{x=\infty} \log_2(1 + a_n P_{\text{peak}} x) f_{g_n}(x) f_{g_p}(y) dx dy \\ &\quad + \int_{y=\frac{I}{P_{\text{peak}}}}^{y=\infty} \int_{x=0}^{x=\infty} \log_2 \left(1 + a_n I \frac{x}{y} \right) f_{g_n}(x) f_{g_p}(y) dx dy \\ &= \frac{1}{\Omega_n \Omega_p} \int_{y=0}^{y=\frac{I}{P_{\text{peak}}}} \int_{x=0}^{x=\infty} \log_2(1 + a_n P_{\text{peak}} x) \exp \left(\frac{-x}{\Omega_n} \right) \\ &\quad \times \exp \left(\frac{-y}{\Omega_p} \right) dx dy \\ &\quad + \frac{1}{\Omega_n \Omega_p} \int_{y=\frac{I}{P_{\text{peak}}}}^{y=\infty} \int_{x=0}^{x=\infty} \log_2 \left(1 + a_n I \frac{x}{y} \right) \exp \left(\frac{-x}{\Omega_n} \right) \\ &\quad \times \exp \left(\frac{-y}{\Omega_p} \right) dx dy \\ &= \frac{1}{\Omega_n \Omega_p \ln 2} \left[\int_{y=0}^{y=\frac{I}{P_{\text{peak}}}} \exp \left(\frac{-y}{\Omega_p} \right) dy \right] \\ &\quad \times \left[\int_{x=0}^{x=\infty} \ln(1 + a_n P_{\text{peak}} x) \exp \left(\frac{-x}{\Omega_n} \right) dx \right] \\ &\quad + \frac{1}{\Omega_n \Omega_p \ln 2} \int_{y=\frac{I}{P_{\text{peak}}}}^{y=\infty} \int_{x=0}^{x=\infty} \ln \left(1 + a_n I \frac{x}{y} \right) \exp \left(\frac{-x}{\Omega_n} \right) \\ &\quad \times \exp \left(\frac{-y}{\Omega_p} \right) dx dy \\ &= \frac{-1}{\ln 2} \left[1 - \exp \left(\frac{-I}{\Omega_p P_{\text{peak}}} \right) \right] \exp \left(\frac{1}{a_n \Omega_n P_{\text{peak}}} \right) \\ &\quad \times \text{Ei} \left(\frac{-1}{a_n \Omega_n P_{\text{peak}}} \right) + \frac{1}{\ln 2} \left[\text{Ei} \left(\frac{-I}{\Omega_p P_{\text{peak}}} \right) - \frac{\Omega_p}{\Omega_p - a_n \Omega_n I} \right] \\ &\quad \times \left\{ \text{Ei} \left(\frac{-I}{\Omega_p P_{\text{peak}}} \right) - \exp \left(\frac{\Omega_p - a_n \Omega_n I}{a_n \Omega_n \Omega_p P_{\text{peak}}} \right) \text{Ei} \left(\frac{-1}{a_n \Omega_n P_{\text{peak}}} \right) \right\} \\ &\quad + \exp \left(\frac{\Omega_p - a_n \Omega_n I}{a_n \Omega_n \Omega_p P_{\text{peak}}} \right) \\ &\quad \times \left\{ \text{Shi} \left(\frac{1}{a_n \Omega_n P_{\text{peak}}} \right) - \text{Chi} \left(\frac{1}{a_n \Omega_n P_{\text{peak}}} \right) \right\} \\ &\triangleq T(a_n \Omega_n). \end{aligned} \tag{60}$$

Similarly, the analytical expression for the second expectation in (23) can be obtained by replacing $a_n \Omega_n$ by Ω , and the analytical expression for the third expectation in (23) can be obtained by replacing Ω_n by Ω in the preceding equation; this completes the proof.

APPENDIX G
PROOF OF THEOREM 7

Using (22) and (27), it follows that

$$\begin{aligned} \mathbb{P}_{\text{out}} &= 1 - \Pr\left(g_n \geq \frac{\xi_n}{P_t^*(g_p)}\right) \Pr\left(g_f \geq \frac{\xi_f}{P_t^*(g_p)}\right) \\ &= 1 - \left\{ \underbrace{\Pr\left(g_n \geq \frac{\xi_n}{P_{\text{peak}}}\right) \Pr\left(g_f \geq \frac{\xi_f}{P_{\text{peak}}}\right) \Pr\left(g_p \leq \frac{I}{P_{\text{peak}}}\right)}_{\mathfrak{X}_1} \right. \\ &\quad \left. + \Pr\left(\frac{g_n}{g_p} \geq \frac{\xi_n}{I}, \frac{g_f}{g_p} \geq \frac{\xi_f}{I}, g_p > \frac{I}{P_{\text{peak}}}\right) \right\}. \quad (61) \end{aligned}$$

Solving for \mathfrak{X}_1 yields

$$\begin{aligned} \mathfrak{X}_1 &= \left[\prod_{u \in \{n, f\}} \int_{\frac{\xi_u}{P_{\text{peak}}}}^{\infty} f_{g_u}(x) dx \right] \left[1 - \exp\left(\frac{-I}{\Omega_p P_{\text{peak}}}\right) \right] \\ &= \left[1 - \exp\left(\frac{-I}{\Omega_p P_{\text{peak}}}\right) \right] \prod_{u \in \{n, f\}} \frac{1}{\Gamma(N_u) \Omega_u^{N_u}} \int_{\frac{\xi_u}{P_{\text{peak}}}}^{\infty} x^{N_u-1} \\ &\quad \times \exp\left(\frac{-x}{\Omega_u}\right) dx \\ &= \left[1 - \exp\left(\frac{-I}{\Omega_p P_{\text{peak}}}\right) \right] \prod_{u \in \{n, f\}} \frac{\Gamma[N_u, \xi_u/(\Omega_u P_{\text{peak}})]}{\Gamma(N_u)}. \quad (62) \end{aligned}$$

The integral above is solved using [22, eqn. (3.381-3), p. 346]. Similarly, solving for \mathfrak{X}_2 yields

$$\begin{aligned} \mathfrak{X}_2 &= \Pr\left(\frac{g_n}{g_p} \geq \frac{\xi_n}{I}, \frac{g_f}{g_p} \geq \frac{\xi_f}{I}, g_p > \frac{I}{P_{\text{peak}}}\right) \\ &= \frac{1}{\Omega_p} \int_{\frac{I}{P_{\text{peak}}}}^{\infty} \exp\left(\frac{-x}{\Omega_p}\right) \Pr\left(g_n \geq \frac{\xi_n}{I} x\right) \Pr\left(g_f \geq \frac{\xi_f}{I} x\right) dx \\ &= \frac{1}{\Omega_p} \int_{\frac{I}{P_{\text{peak}}}}^{\infty} \exp\left(\frac{-x}{\Omega_p}\right) \left[1 - F_{g_n}\left(\frac{\xi_n}{I} x\right)\right] \left[1 - F_{g_f}\left(\frac{\xi_f}{I} x\right)\right] dx \\ &= \frac{1}{\Omega_p} \int_{\frac{I}{P_{\text{peak}}}}^{\infty} \exp\left(\frac{-x}{\Omega_p}\right) \exp\left(\frac{-\xi_n x}{\Omega_n I}\right) \sum_{l=0}^{N_n-1} \frac{1}{l!} \left(\frac{\xi_n x}{\Omega_n I}\right)^l \\ &\quad \times \exp\left(\frac{-\xi_f x}{\Omega_f I}\right) \sum_{k=0}^{N_f-1} \frac{1}{k!} \left(\frac{\xi_f x}{\Omega_f I}\right)^k dx \\ &= \frac{1}{\Omega_p} \sum_{k=0}^{N_f-1} \sum_{l=0}^{N_n-1} \frac{\xi_n^l \xi_f^k}{k! l! \Omega_n^l \Omega_f^k I^{k+l}} \int_{\frac{I}{P_{\text{peak}}}}^{\infty} x^{k+l} \\ &\quad \times \exp\left[-\left(\frac{1}{\Omega_p} + \frac{\xi_n}{\Omega_n I} + \frac{\xi_f}{\Omega_f I}\right) x\right] dx \\ &= \frac{1}{\Omega_p} \sum_{k=0}^{N_f-1} \sum_{l=0}^{N_n-1} \Gamma\left[k+l+1, \left(\frac{1}{\Omega_p} + \frac{\xi_n}{\Omega_n I} + \frac{\xi_f}{\Omega_f I}\right) \frac{I}{P_{\text{peak}}}\right] \\ &\quad \times \frac{\xi_n^l \xi_f^k}{k! l! \Omega_n^l \Omega_f^k I^{k+l}} \left(\frac{1}{\Omega_p} + \frac{\xi_n}{\Omega_n I} + \frac{\xi_f}{\Omega_f I}\right)^{-(k+l+1)}. \quad (63) \end{aligned}$$

The integral above is solved using [22, eqn. (3.381-3), p. 346]. Therefore, using (61)-(63), an analytical expression for (27) is given by (28); this concludes the proof.

REFERENCES

[1] M. Nekovee, "Opportunities and enabling technologies for 5G and beyond-5G spectrum sharing," in *Handbook of Cognitive Radio*, W. Zhang, Ed. Singapore: Springer, 2018, pp. 1–15.

[2] A. Goldsmith, S. A. Jafar, I. Maric, and S. Srinivasa, "Breaking spectrum gridlock with cognitive radios: An information theoretic perspective," *Proc. of the IEEE*, vol. 97, no. 5, pp. 894–914, 2009.

[3] Z. Qin and G. Y. Li, "Pathway to intelligent radio," *IEEE Wireless Commun.*, vol. 27, no. 1, pp. 9–15, 2020.

[4] P. Zhu, J. Li, D. Wang, and X. You, "Machine-learning-based opportunistic spectrum access in cognitive radio networks," *IEEE Wireless Commun.*, vol. 27, no. 1, pp. 38–44, 2020.

[5] M. Vaezi, Z. Ding, and H. Poor, *Multiple Access Techniques for 5G Wireless Networks and Beyond*. Cham, Switzerland: Springer International Publishing, 2018.

[6] M. Vaezi, R. Schober, Z. Ding, and H. V. Poor, "Non-orthogonal multiple access: Common myths and critical questions," *IEEE Wireless Commun.*, vol. 26, no. 5, pp. 174–180, 2019.

[7] Y. Tian, G. Pan, and M.-S. Alouini, "On NOMA-based mmWave communications," *arXiv preprint arXiv:2009.07221*, 2020.

[8] L. Lv, Q. Ni, Z. Ding, and J. Chen, "Application of non-orthogonal multiple access in cooperative spectrum-sharing networks over Nakagami- m fading channels," *IEEE Trans. Veh. Technol.*, vol. 66, no. 6, pp. 5506–5511, 2017.

[9] M. F. Kader, M. B. Shahab, and S. Y. Shin, "Cooperative spectrum sharing with energy harvesting best secondary user selection and non-orthogonal multiple access," in *Int. Conf. Computing, Net. Commun. (ICNC)*, 2017, pp. 46–51.

[10] B. Chen, Y. Chen, Y. Chen, Y. Cao, N. Zhao, and Z. Ding, "A novel spectrum sharing scheme assisted by secondary NOMA relay," *IEEE Wireless Commun. Lett.*, vol. 7, no. 5, pp. 732–735, 2018.

[11] M. F. Kader, "A power-domain NOMA based overlay spectrum sharing scheme," *Future Generation Computer Systems*, vol. 105, pp. 222 – 229, 2020.

[12] X. Zhang, D. Guo, K. An, Z. Chen, B. Zhao, Y. Ni, and B. Zhang, "Performance analysis of NOMA-based cooperative spectrum sharing in hybrid satellite-terrestrial networks," *IEEE Access*, vol. 7, pp. 172 321–172 329, 2019.

[13] L. Lv, J. Chen, Q. Ni, Z. Ding, and H. Jiang, "Cognitive non-orthogonal multiple access with cooperative relaying: A new wireless frontier for 5G spectrum sharing," *IEEE Commun. Mag.*, vol. 56, no. 4, pp. 188–195, 2018.

[14] Y. Liu, Z. Ding, M. El-kashlan, and J. Yuan, "Nonorthogonal multiple access in large-scale underlay cognitive radio networks," *IEEE Trans. Veh. Technol.*, vol. 65, no. 12, pp. 10 152–10 157, 2016.

[15] S. Arzykulov, T. A. Tsiftsis, G. Nauryzbayev, M. Abdallah, and G. Yang, "Outage performance of underlay CR-NOMA networks with detect-and-forward relaying," in *IEEE Global Commun. Conf. (GLOBECOM)*, 2018, pp. 1–6.

[16] S. Arzykulov, T. A. Tsiftsis, G. Nauryzbayev, and M. Abdallah, "Outage performance of cooperative underlay CR-NOMA with imperfect CSI," *IEEE Commun. Lett.*, vol. 23, no. 1, pp. 176–179, 2019.

[17] D.-T. Do, A.-T. Le, , and B. M. Lee, "On performance analysis of underlay cognitive radio-aware hybrid OMA/NOMA networks with imperfect CSI," *Electronics*, vol. 8, no. 7, p. 819, July 2019.

[18] V. Kumar, B. Cardiff, and M. F. Flanagan, "Fundamental limits of spectrum sharing for NOMA-based cooperative relaying under a peak interference constraint," *IEEE Trans. Commun.*, vol. 67, no. 12, pp. 8233–8246, 2019.

[19] S. Arzykulov, G. Nauryzbayev, T. A. Tsiftsis, B. Maham, M. S. Hashmi, and K. M. Rabie, "Underlay spectrum sharing for NOMA relaying networks: Outage analysis," in *Int. Conf. Computing, Net. Commun. (ICNC)*, 2020, pp. 897–901.

[20] L. Sboui, Z. Rezki, and M. Alouini, "Achievable rate of spectrum sharing cognitive radio systems over fading channels at low-power regime," *IEEE Trans. Wireless Commun.*, vol. 13, no. 11, pp. 6461–6473, 2014.

[21] Z. Ding, H. Dai, and H. V. Poor, "Relay selection for cooperative NOMA," *IEEE Wireless Commun. Lett.*, vol. 5, no. 4, pp. 416–419, 2016.

[22] A. Jeffrey and D. Zwillinger, *Table of Integrals, Series, and Products*, 7th ed. Cambridge, MA, USA: Elsevier Science, 2007.

[23] F. Olver, D. Lozier, R. Boisvert, and C. Clark, *NIST Handbook of Mathematical Functions Handbook*. Cambridge University Press, 2010.

[24] V. S. Adamchik and O. I. Marichev, "The algorithm for calculating integrals of hypergeometric type functions and its realization in REDUCE system," in *Proc. Int. Symp. Symbolic and Algebraic Comp.* New York, NY, USA: ACM, 1990, pp. 212–224.